applied sciences

MDPI

Article

Application of Satellite-Derived Summer Bloom Indicators for Estonian Coastal Waters of the Baltic Sea

Ian-Andreas Rahn [1], Kersti Kangro [1,2], Andres Jaanus [3] and Krista Alikas [1,*]

[1] Tartu Observatory, University of Tartu, Observatooriumi 1, 61602 Tõravere, Estonia; ian-andreas.rahn@ut.ee (I.-A.R.); kersti.kangro@ut.ee (K.K.)
[2] Centre for Limnology, Estonian University of Life Sciences, Limnoloogia tee 1, 61117 Vehendi küla, Estonia
[3] Estonian Marine Institute, University of Tartu, Mäealuse 14, 12618 Tallinn, Estonia; andres.jaanus@ut.ee
* Correspondence: krista.alikas@ut.ee

Abstract: The aim of this study was to test and develop the indicators for the remote sensing assessment of cyanobacterial blooms as an input to the estimation of eutrophication and the environmental status (ES) under the Marine Strategy Framework Directive (MSFD) in the optically varying Estonian coastal regions (the Baltic Sea). Here, the assessment of cyanobacteria blooms considered the chlorophyll-a (chl-a), turbidity, and biomass of N_2-fixing cyanobacteria. The Sentinel-3 A/B Ocean and Land Colour Instrument (OLCI) data and Case-2 Regional CoastColour (C2RCC) processor were used for chl-a and turbidity detection. The ES was assessed using four methods: the Phytoplankton Intensity Index (PII), the Cyanobacterial Surface Accumulations Index (CSA), and two variants of the Cyanobacterial Bloom Indicator (CyaBI) either with in situ-measured cyanobacterial biomass or with satellite-estimated cyanobacterial biomass. The threshold values for each coastal area ES assessment are presented. During 2022, the NW Gulf of Riga reached good ES, but most of the 16 coastal areas failed to achieve good ES according to one or multiple indices. Overall, the CyaBI gives the most comprehensive assessment of cyanobacteria blooms, with the CyaBI (in situ) being the best suited for naturally turbid areas. The CyaBI (satellite) could be more useful than in situ in large open areas, where the coverage of in situ sampling is insufficient.

Keywords: Baltic Sea; OLCI; cyanobacteria bloom indices; marine strategy framework directive; MSFD; environmental status

check for updates

Citation: Rahn, I.-A.; Kangro, K.; Jaanus, A.; Alikas, K. Application of Satellite-Derived Summer Bloom Indicators for Estonian Coastal Waters of the Baltic Sea. *Appl. Sci.* **2023**, *13*, 10211. https://doi.org/10.3390/app131810211

Academic Editor: Vicente Mariscal

Received: 31 July 2023
Revised: 31 August 2023
Accepted: 9 September 2023
Published: 11 September 2023

Copyright: © 2023 by the authors. Licensee MDPI, Basel, Switzerland. This article is an open access article distributed under the terms and conditions of the Creative Commons Attribution (CC BY) license (https://creativecommons.org/licenses/by/4.0/).

1. Introduction

The Baltic Sea is a semi-enclosed sea bordering nine countries: Denmark, Sweden, Finland, Russia, Estonia, Latvia, Lithuania, Poland, and Germany. The sea provides economic benefits from tourism to fishing [1]. Simultaneously, it is under heavy anthropogenic pressure from nearby industries, cities, agriculture, and other inputs from various human activities. An enrichment of nutrients results in an increase in the eutrophication of the sea [2]. This, in turn, has cascading impacts on the local ecosystem from an increase in primary production, and changes in the metabolism of organisms, to oxygen depletion, which has led to changes in food webs and benthic and planktic communities [3,4]. The increased nutrient load into the sea has led to an increase in phytoplankton biomass, including cyanobacteria. Furthermore, cyanobacteria can cope with nitrogen limitation by fixing atmospheric nitrogen, providing additional nutrient inputs to an already nutrient-rich system [5]. It has been reported that spatial and temporal parameters of harmful algal blooms (HABs) have shifted [6]. The blooms are beginning earlier and cover a larger area than previously [7–9]. HABs in the Baltic Sea consist of both non-toxic and toxic cyanobacteria species and can be a nuisance to local aquatic ecosystems and maritime industry and pose a threat to public health [10–12]. Contact with different toxin-producing species of cyanobacteria can lead to skin irritation, liver damage, or paralysis [13]. In Estonian coastal areas, estuarine species such as the *Aphanizomenon flos-aquae* and *Nodularia* species

are prevalent and dominate during the summer HAB events [14], whereas bloom-forming cyanobacteria, especially *Nodularia spumigena*, and *Dolichospermum* spp., all may produce toxins [15].

Currently, in situ measurements taken sparsely and from singular measuring points are used to give an indication of the environmental status (ES) of the entire coastal area. This is problematic as the coastal areas differ from one another regarding currents, wind speed, and prevailing direction, as well as the species present (e.g., presence of vacuoles in some species), and as a result, HABs are not homogenous across the coast. Numerous problems arise from in situ sampling of cyanobacterial biomass. Using research vessels to gather water samples leads to unintended disturbances in the horizontal and vertical distribution of cyanobacteria [16]. Satellite images could provide a solution to monitoring large-scale cyanobacterial blooms [17,18]. Satellites allow for much larger areas to be measured at much more frequent timescales (daily without cloud cover) [19]. This would permit the identification of possible parameters responsible for changes in time and space. However, the downside to using satellite data is that it can only give information about the surface of the waterbody, whereas cyanobacteria are mixed in the water column and extensive subsurface blooms can occur [20]. This is one of the reasons for match-up inconsistencies, as in situ measurements follow different methodologies and, in some instances, consider biomass in deeper layers of the water column, which satellite images cannot pick up. Furthermore, depending on the satellite, the large spatial resolution of Sentinel-3, for example, and even Sentinel-2 and Landsat, do not allow for monitoring the spatial distribution at very fine scales. This can be an issue, as Kutser (2004) has shown, as blooms can be patchy and differ at even 30 m scales in the Baltic Sea. One solution is ground-based remote sensing, as evidenced by Cook et al. [21], but this is better suited for smaller water bodies such as lakes and would not be fiscally viable for coastal areas. Currently, another issue is the inability to detect specific toxins or toxin-producing species via satellite images which hinders the usefulness of satellite data for the more accurate monitoring of blooms [22,23]. Despite all of it, satellite remote sensing is a useful tool for monitoring large-scale bloom events through time and space.

Monitoring the ES of coastal areas is required under the EU Water Framework Directive (WFD) [24]. Furthermore, monitoring and managing aquatic resources is necessary to ensure the safety of marine environments and is one of the key parameters under the United Nations' Sustainable Development Goal 6 [25]. Under the Marine Strategy Framework Directive (MSFD) (2008) of the European Commission, it is a priority for countries in the EU to monitor the ES of their waterbodies and achieve a good environmental state. One of the key parameters which must be monitored is eutrophication as it can lead to numerous cascading environmental impacts, such as ecosystem deterioration, cyanobacterial blooms, and anaerobic conditions of the benthic layers [26]. The Baltic Marine Environment Protection Commission, also known as the Helsinki Commission or HELCOM, is the organization responsible for implementing the principles of the MSFD in the Baltic Region and has coordinated the development of indicators for monitoring the ES of the region. Each HELCOM indicator evaluates a specific aspect of the Baltic Sea. The HELCOM indicators go through three stages: the candidate indicator, the pre-core indicator, and the core indicator. An indicator is officially approved when it fulfils rigorous criteria, for example, it has approved threshold values and data availability. An issue with using indicators to describe environmental processes is that they are difficult to develop for complex biological phenomena. The intricacies of bloom events and their associated relationship within food webs, as well as the lack of spatially and temporally extensive data, make assessing ES complicated [17,27,28]. Among other indicators for assessing ES, ranging from acidification and beach litter to seal reproduction and trout abundance, is the pre-core indicator Cyanobacterial Bloom Index (CyaBI) [4,29]. The CyaBI consists of two inputs: the remote sensing (RS) data of bloom parameters and in situ cyanobacterial biomass [17]. Other indices, outside of HELCOM, have also been used in the Baltic Sea to assess bloom

events: Cyanobacterial Surface Accumulation (CSA) [17] and the Phytoplankton Intensity Index [30], among others [8,31,32].

Cyanobacterial methods for setting target levels and assessing the blooms typically make use of chlorophyll-a concentrations (chl-a) [28]. Bloom assessment methods, such as CSA, the CyaBI, and the Phytoplankton Intensity Index, have been shown to be applicable to different open sea areas of the Baltic Sea [17,30]. Additionally, band differences for the bands of the Ocean and Land Colour Instrument (OLCI) and bands of the Moderate Resolution Imaging Spectroradiometer (MODIS) were shown to agree with the in situ data in the Baltic Sea and could be used for the detection of cyanobacteria blooms [33]. Other approaches, such as hyperspectral satellites [34] or unmanned aerial vehicles (UAVs) [35,36], have also been used in other parts of the world. However, to our knowledge, no previous research has applied these methods to the Estonian coast. The Estonian coastal waters are optically complex and heavily influenced by colored dissolved organic matter (CDOM) and total suspended matter (TSM) and are typically shallow, which have made it an optically difficult area to study via satellites. When estimating a baseline for ES, it is important to consider that the Baltic Sea has historically seen phytoplankton blooms even before human intervention. As highlighted by HELCOM, a threshold ES should therefore not be set as "no blooms present" but rather should ensure that blooms are not severe and do not cause economic and ecological harm. Simultaneously, the assessment should be in accordance with the sustainable use of sea resources by humans [37]. Previously, a time-series analysis based on the satellite data of cyanobacterial blooms in the Baltic Sea has been conducted by, e.g., Kahru and Elmgren [8], where the idea of a lack of a bloom-free period was solidified.

The main objective of this research was to test various indices used to monitor the ES of Estonian coastal areas in regard to cyanobacteria biomass and to assess the applicability of input parameters such as the chl-a, turbidity, and cyanobacteria biomass, derived from Sentinel-3 OLCI data products. Through the use of indices, an assessment of the current cyanobacterial biomass in the Baltic Sea during the summer bloom events from 2016 to 2022 using satellite data was made.

2. Materials and Methods

2.1. Study Area

The Estonian coastal sea is divided into 16 water bodies: Gulf of Riga (Northwest, Northeast, center), Pärnu Bay, Hara and Kolga bays, Hiiu Shallow, Matsalu Bay, Haapsalu Bay, Moonsund Sea, Eru-Käsmu Bay, Muuga-Tallinna-Kakumäe Bay, Kassari-Õunaku Bay, Narva-Kunda Bay, Soela Strait, Pakri bays, and Kihelkonna Bay (Table 1 and Figure 1) [38,39]. The varying environmental states of the different areas have led to contrasting cyanobacterial bloom conditions.

Narva-Kunda Bay and Eru-Käsmu Bay are open areas in the southeastern Gulf of Finland. Narva-Kunda Bay is heavily influenced by currents and waves. Rivers are the main sources of pollution from heavy industry in the adjacent areas. Due to the lack of human activity and freshwater inflow, Eru-Käsmu is much less polluted.

The Hara–Kolga, Muuga-Tallinna-Kakumäe, and Pakri bays are all semi-enclosed shallow bays with deeper parts of the sea open to waves and currents. The influence of fresher and nutrient-rich water from the open part of the Gulf of Finland can also occur. The main sources of pollution in these areas are the city of Tallinn and maritime traffic.

Hiiu Shallow, Kihelkonna Bay, and Soela Strait can be described as being strongly influenced by the Baltic Sea due to their openness. These areas are minimally impacted by the adjacent land.

Haapsalu Bay is mostly shallow and semi-enclosed. The area is under the influence of effluents from the coastal city of Haapsalu. Due to poor water exchange, nutrients also accumulate in the inner part of the bay.

Table 1. Names and environmental parameters of the study areas. Median summer chl-a is given, minimum and maximum in brackets. Average salinity is given as the range of values between different sampling stations in a coastal area (April–October).

Coastal Area	Chl-a (In Situ) mg m^{-3}	Frequency of In Situ Sampling		Average Salinity, psu	Predominant Depth Range, m
		Average Number of Sampling per Year	Minimum Years between Measurements		
Narva-Kunda Bay	5.7 (0.7–29.5)	5.4	0	4–5	5–25
Eru-Käsmu Bay	5.1 (1.8–32.1)	4.0	1	4.5–5	20–50
Hara and Kolga bays	3.8 (0.2–20.3)	4.4	0	5–5.5	25–80
Muuga-Tallinna-Kakumäe Bay	4.0 (0.2–18.0)	11.6	0	5.5–6	20–50
Pakri bays	4.5 (0.7–8.4)	7	6	5.5–6.5	10–50
Hiiu Shallow	3.5 (1.8–7.7)	6	6	6–7	10–25
Haapsalu Bay	3.5 (0.9–9.1)	4.5	2	3–6	1–3
Matsalu Bay	2.8 (1.5–6.3)	4	6	3–6	1–3
Soela Strait	2.7 (1.1–6.6)	5	6	6.5–7	20–50
Kihelkonna Bay	1.9 (0.8–4.9)	5	6	6.5–7	10–25
Pärnu Bay	7.7 (2.9–47.7)	5.3	0	4–5	3–5
Kassari-Õunaku Bay	1.8 (0.8–6.8)	5.5	2	6–7	3–7
Moonsund Sea	2.4 (0.3–5.8)	3.3	2	5.5–6.5	5–10
Gulf of Riga (NW)	NA *	NA *	NA *	5.5–6.5	10–25
Gulf of Riga (NE)	8.7 (2.2–71.9)	5.1	0	5–5.5	10–20
Gulf of Riga (central)	3.1 (1.4–5.7)	2.8	1	5–5.5	25–40

* Sampling started in 2022.

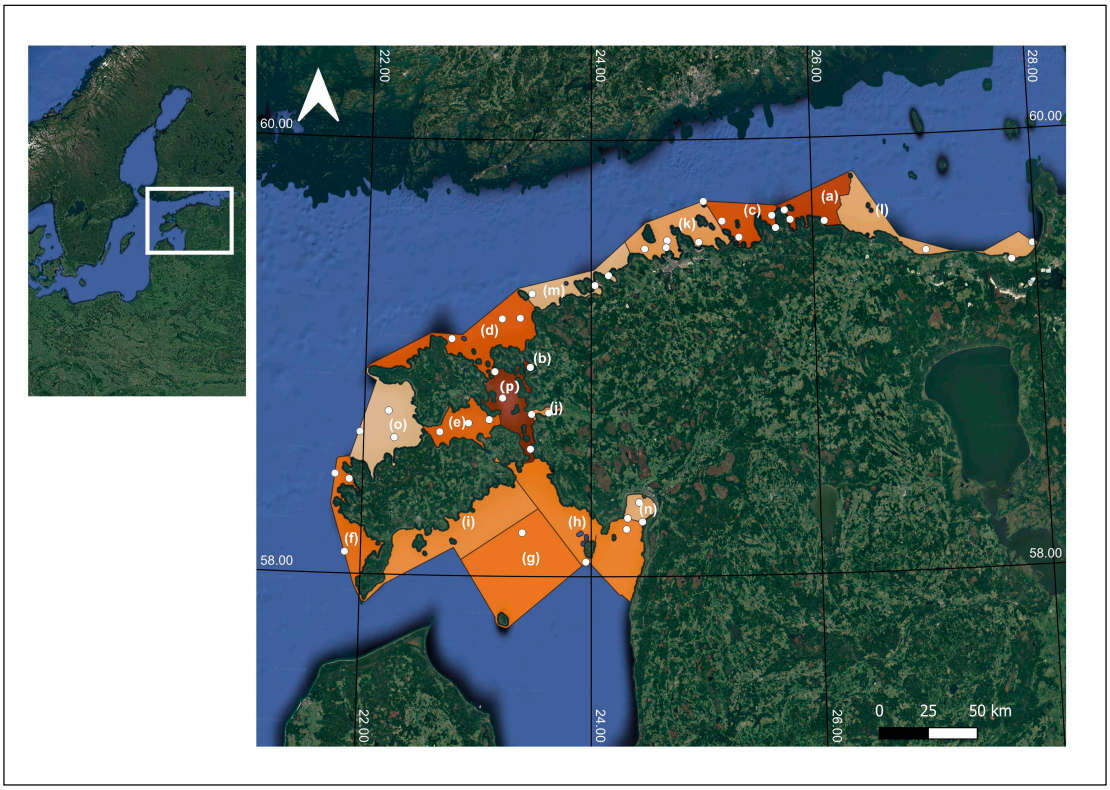

Figure 1. Coastal areas of Estonia and in situ sampling locations are represented as white points. (a) Eru-Käsmu Bay, (b) Haapsalu Bay, (c) Hara and Kolga bays, (d) Hiiu Shallow, (e) Kassari-Õunaku Bay, (f) Kihelkonna Bay, (g) Gulf of Riga (central), (h) Gulf of Riga (NE), (i) Gulf of Riga (NW), (j) Matsalu Bay, (k) Muuga-Tallinna-Kakumäe Bay, (l) Narva-Kunda Bay, (m) Pakri bays, (n) Pärnu Bay, (o) Soela Strait, (p) Moonsund Sea. Base image: Google Hybrid.

Matsalu Bay is a typical estuary where fresh water in the eastern part transitions to brackish water (5–6 PSU) at the mouth of the bay.

Kassari-Õunaku Bay is open from the west, while the eastern side is separated from the neighboring water bodies by an archipelago.

In the Moonsund Sea, active north–south currents affect the physicochemical properties of the water body.

The Gulf of Riga is influenced by the inflow from a huge drainage area, mostly entering the southern and eastern parts, and by water exchange with the open Baltic Sea through the Irbe Strait.

Pärnu Bay is shallow and strongly impacted by waves and currents causing bottom sediments to move easily during storm events. Pärnu River is also a source of large amounts of suspended solids and nutrients [40]. Additionally, the pollution load is also strongly influenced by the city of Pärnu.

2.2. Data Sets

In situ data were gathered by the Estonian Marine Institute in the frame of the national monitoring program. The measurements of the chl-a and cyanobacterial biomass were performed according to the HELCOM guidelines (phytoplankton [41] and chl-a [42]) for the period of 2016–2022. Chl-a was measured spectrophotometrically, using extraction in 96% ethanol and calculation according to Arvola, 1981. The in situ sampling points in the various coastal areas are given in Figure 1. The depth of the measurements ranged from 0 m (on the surface) to 10 m under the surface. The temperature measurements were obtained from the Estonian Environment Agency which were taken at various ports across the coastline.

For satellite data, Sentinel-3A/B OLCI Level-1 full-resolution data were used. For validation, the satellite data were gathered from April to September. At higher latitudes, it is not possible to viably use satellite data due to the sun's angle earlier in the year which disperses incoming solar irradiance onto a larger area, decreasing the energy per unit area. In situ data were used to validate the chl-a of the two processors C2RCC and POLYMER. POLYMER is an atmospheric correction model based on spectral matching. It uses a polynomial to model the spectral reflectance of the atmosphere, a water reflectance model, and all available spectral bands in the visible spectral region [43]. C2RCC is a neural-network-based atmospheric correction processor which provides the results of water-leaving reflectance (ρ_w), inherent optical properties (IOPs), chl-a, and total suspended matter (TSM) [44,45]. Here, the chl-a outputs (chl_conc product) of C2RCC were used. The pixel flags are given in Table 2. The monthly temperatures were averaged and, along with a salinity of 5 PSU, were used as input for the Case-2 Regional CoastColour processor (C2RCC) v1.9.

Table 2. The flags used to exclude pixels for C2RCC and include pixels for POLYMER.

Flags Used with C2RCC	Flags Used with POLYMER
IDEPIX_CLOUD	bitmask = 0
IDEPIX_BRIGHT	bitmask = 1024
IDEPIX_CLOUD_SHADOW	
IDEPIX_CLOUD_AMBIGUOUS	
IDEPIX_CLOUD_SURE	
IDEPIX_CLOUD_BUFFER	
Cloud_risk	
quality_flags.bright	
quality_flags.straylight_risk	
quality_flags.invalid	
quality_flags.sun_glint_risk	

Validation of the satellite data was performed according to the Sentinel-3 validation recommendations [46]. A minimum number of valid pixels were chosen to be at least 50% for each 3 × 3 window. Although not in the recommendations of the S3VT, in order to consider more data points, a maximum 12 h difference in time was chosen. The pixel outliers were removed according to the mean and standard deviation (SD) of the results following the filtration methods in the recommendations, and the values within a coefficient of variation of 20% were used. The correlation was estimated based on the coefficient of determination and Pearsons's correlation coefficient.

2.3. Clustering

A clustering analysis was performed to assess possible similarities in the time series of the chl-a and turbidity values of the 16 coastal areas. The analysis was based on the K-means clustering of the time series. The time series consisted of continuous daily satellite-derived chl-a and turbidity data from April to September of the year 2022. In order to obtain a continuous time series, a 7-day average was used.

2.4. Bloom Indices

Summer blooms were characterized by 3 different indices. An overview of the used indices and necessary inputs is given in Figure 2.

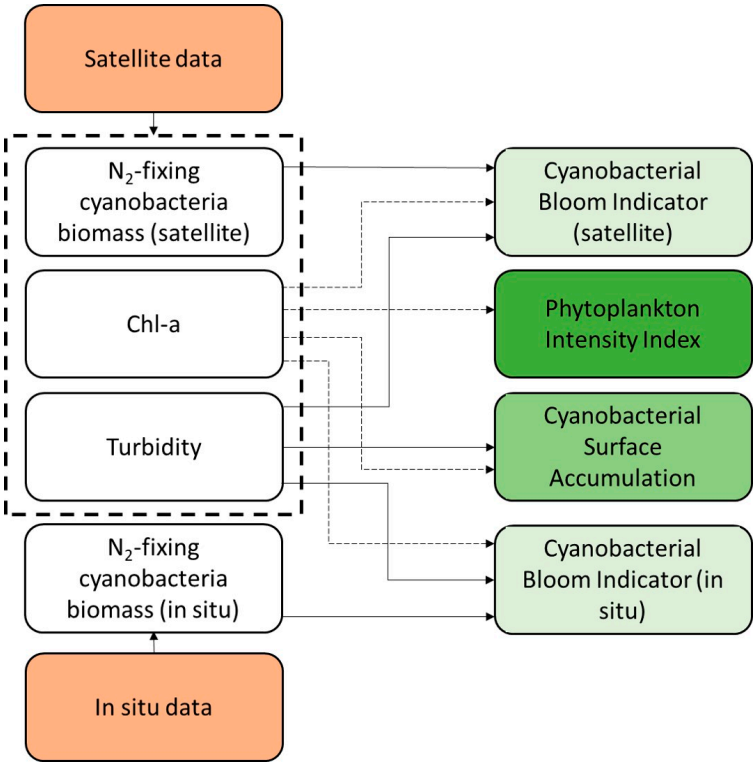

Figure 2. Schematic overview of the inputs used for the different indices. Orange color represents sources of inputs, green colors represent different indices.

2.4.1. Phytoplankton Intensity Index (PII)

The Phytoplankton Intensity Index was initially designed by Fleming and Kaitala [30] to assess the spring bloom events in the Baltic Sea. The index is based on summing chl-a (Figure 2) values exceeding a certain threshold. To overcome data gaps due to cloud cover, a 7-day running average of chl-a was calculated based on the mean chl-a of each coastal area on a daily basis. A threshold concentration of 5 mg m^{-3} was used to assess the beginning

of a bloom event. The intensity index was calculated by approximating a time-intensity integral for time periods when the threshold value was exceeded.

$$PII = \sum_{i=1}^{n} h_i \quad (1)$$

where i is the day, n is the number of bloom days, and h_i is the 7-day running average of chl-a.

2.4.2. Cyanobacterial Surface Accumulation (CSA) Index

Cyanobacterial bloom indicator methods have been developed by and are thoroughly described by Anttila et al. [17]. In order to obtain a CSA value, firstly, an algal barometer (AB) value was calculated based on the weighted sum of the proportion of positive algae bloom estimations. The algal bloom estimates were divided into 4 groups, with 1–3 being considered as positive: 0—no algae, 1—some algae, 2—abundant algae, and 3—very abundant algae,

$$AB = \frac{1}{n_{tot}}(n_{\#cl1} + n_{\#cl2} \times 2 + n_{\#cl3} \times 3) \quad (2)$$

where n_{tot} is the total number of pixels with algal values, and $n_{\#cl1–\#cl3}$ are the number of pixels in a specific class, respectively.

The grouping was made on the basis of the chl-a (threshold 5 mg m^{-3} was used differently from Anttila et al. [14]) and turbidity (Table 3 and Figure 2). The turbidity was calculated according to Kyryliuk et al. [47].

Table 3. Grouping conditions for estimating AB. Chl-a values are in mg m^{-3} and turbidity in FNU.

Group	Chl-a	Turbidity
0—no algae	<5	<2.5
1—some algae	5–11	2.5–4.5
2—abundant algae	11–27	4.5–7.5
3—very abundant	>27	>7.5

Secondly, an empirical cumulative distribution function (ECDF) was calculated based on the AB values [17]. Three bloom parameters, the seasonal bloom volume, intensity, and duration, were derived from the ECDF. The indicative parameters were then normalized and averaged to obtain the CSA index.

$$P_{norm,y} = (P_y - P_{max})/(P_{min} - P_{max}) \quad (3)$$

where $P_{norm,y}$ is the normalized value for one of the three parameters (volume, intensity, and duration) in the year y, P_y is the parameter value, and P_{max} and P_{min} are the maximum and minimum values of the time series for the period 2016–2021. The CSA index forms one part of the CyaBI index [37].

2.4.3. Cyanobacterial Bloom Indicator (CyaBI)

As an additional step for the indicator, the CSA index was supplemented with in situ cyanobacterial biomass measurements in order to obtain the CyaBI index as described by Anttila et al. [17]. The part of the cyanobacterial biomass being an input for the CyaBI was calculated as the sum of three genera of the nitrogen-fixing and bloom-forming cyanobacteria: *Aphanizomenon*, *Nodularia*, and *Dolichospermum* [29]. The in situ biomass data were obtained from the Estonian Marine Institute monitoring of Estonian coastal areas, whereas the satellite-derived biomass was estimated from the Maximum Chlorophyll Index (MCI) values. The MCI is a line-height algorithm originally developed for MERIS [48], but due to spectral band continuity, it is also applicable to the OLCI [49]. Line-height algorithms are generally useful for estimating cyanobacterial blooms in optically complex waters because they are less hindered by issues of atmospheric corrections [50] as the MCI estimates chl-a from Level 1 satellite data. The MCI is not sensitive in waters where the chl-a is low

(<10 mg m^{-3}) as reported by Binding et al. (2013) [51] but functions well in waters with high chl-a. The CyaBI consists of the normalized value of the two parameters, in situ cyanobacteria biomass and satellite-derived CSA. After normalization, an average of the two parameters is taken as the value for the CyaBI.

2.5. Environmental Status Thresholds

To assess the current environmental status of the coastal areas, a threshold value needs to be identified. A common approach to calculating a threshold is to take the 75th percentile of the time-series values as an indicator of "good environmental status" [52–55]. Here, we have used the same approach. For each coastal area, the threshold value for the year 2022 was taken as the 75th percentile of the years 2016–2021 values for each index and coastal area. Although the official reporting period is 6 years, 2016–2022, we wanted to also give an assessment of the most recent environmental status, so the year 2022 was chosen.

3. Results

Firstly, the input parameters required by different indices, such as the chl-a, turbidity, and N_2-fixing cyanobacteria biomass, are analyzed. The differences between the in situ and satellite-derived data are highlighted. The results of the various indices are presented, and comparisons are made. Finally, the ES of the 16 coastal water bodies in 2022 is presented.

3.1. Input Parameters for Estimating Bloom Indicators

3.1.1. Chl-a and Turbidity

Most of the in situ measurements showed chl-a in the range of 3.0–7.3 mg m^{-3} (interquartile range IQR), whereas the satellite data showed a larger variation in the chl-a, 2.9–15.6 mg m^{-3} (Figure 3). The satellite-derived turbidity had a range of values from 0.3 to 5.4 FNU (Figure 3). The Haapsalu, Matsalu, and Pärnu bays showed much higher chl-a and turbidity than the other coastal areas. No apparent linear relationship between chl-a and turbidity was found in most of the coastal areas (Appendix B, Figure A2). This is even more evident when looking at the chl-a and turbidity throughout the phytoplankton spring and summer bloom period of April–September. Looking at the chl-a time series, differences between the three bays from each other and from the other areas can be observed (clusters 1, 2, and 3 in Figure 4). The peak in chl-a was observed in June in Matsalu Bay (cluster 3) but toward the end of August in Haapsalu Bay (cluster 1). Cluster 4, which included all the other coastal areas, did not exceed 10 mg m^{-3} chl-a in 2022 (Figure 4). This suggests that a one-size-fits-all approach to estimating ES is not applicable to all coastal water bodies when basing it on chl-a and turbidity. The annual peak of chl-a in Pärnu Bay likely occurs in the early spring as the chl-a is already highest in April and shows a downward trend from then on.

According to the turbidity, the coastal areas were divided into six clusters (Figure 5). Clusters 3 and 5 showed low turbidity throughout the time series. In clusters 1 and 6, the areas were more turbid during the spring and early summer. Cluster 4, which includes the Pärnu and Matsalu bays, showed a peak in turbidity before the start of our observation period which likely stems from higher river inputs during the early spring as a result of snowmelt. However, a second turbidity peak appeared at the end of the summer. Cluster 2, which exclusively included Haapsalu Bay, showed the highest turbidity values as well as the largest seasonal variability. There was a clear peak in May and another, even higher peak, at the end of August (Figure 4). The peak at the end of the summer is in accordance with a chl-a peak a few days before. This could be a possible indication of a significant bloom event in Haapsalu Bay in 2022 (Figure 4 cluster 1 and Figure 5 cluster 2).

Figure 6 shows the comparison of the C2RCC and POLYMER estimated chl-a and the measured in situ chl-a. The C2RCC validation resulted in a total of 135 valid chl-a match-ups and only 46 for POLYMER. Both processors showed a weak relationship: C2RCC $R^2 = 0.2$ ($r = 0.45$, $df = 133$, $p < 0.05$), and POLYMER $R^2 = 0.39$ ($r(41) = 0.64$, $p < 0.05$) (Figure 6). Similarly, previous research has also shown a poor correlation between the AC algorithms in the Baltic Sea [56,57]. Although POLYMER showed a better relationship,

there were fewer match-ups compared to C2RCC. Previous work has also suggested that for the Baltic Sea region, C2RCC is the best available processor for chl-a estimates [58]. Because of these reasons, it was decided to proceed with the C2RCC data products.

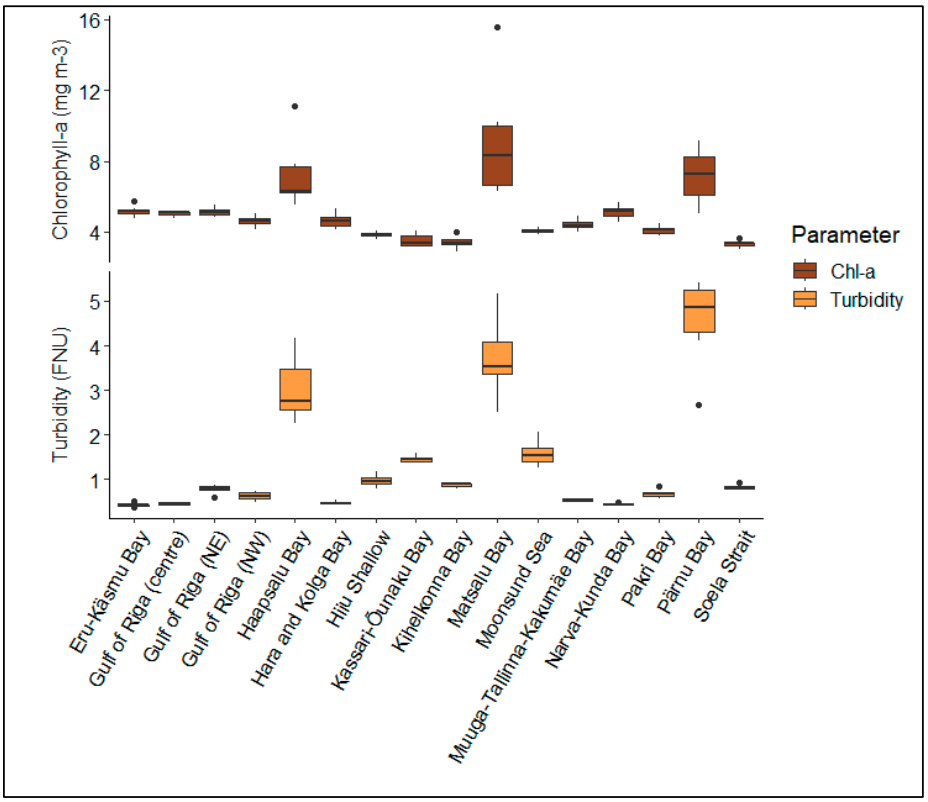

Figure 3. Satellite-derived chl-a (mg m^{-3}) and turbidity (FNU) in coastal areas in 2016–2022. Boxes represent interquartile range (IQR), middle line represents median, whiskers show the maximum and minimum values, and black dots represent outliers.

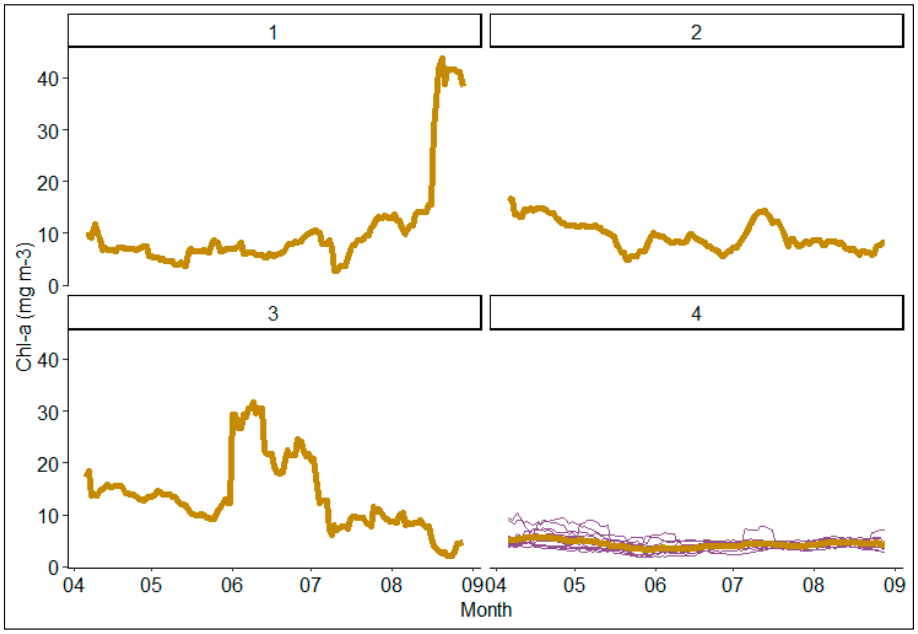

Figure 4. K-means clustering of coastal areas based on daily chl-a in 2022 from April to September. Centroids are given in yellow. Cluster 1: Haapsalu Bay; Cluster 2: Pärnu Bay; Cluster 3: Matsalu Bay; Cluster 4: all coastal areas except for the three mentioned in other clusters.

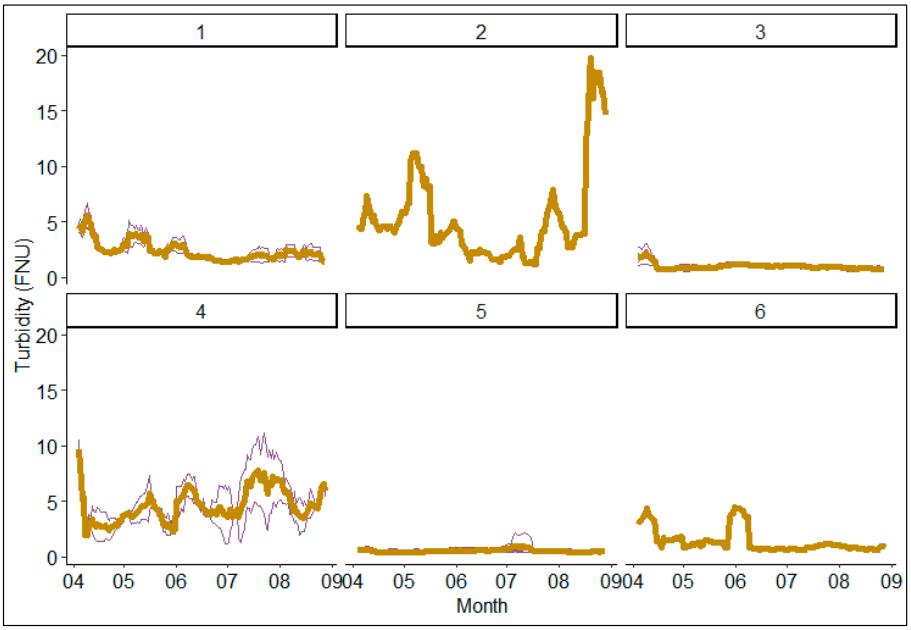

Figure 5. K-means clustering of coastal areas based on daily turbidity in 2022 from April to September. Centroids are given in yellow. Cluster 1: Kassari-Õunaku Bay and Moonsund Sea; Cluster 2: Haapsalu Bay; Cluster 3: Hiiu Shallow, Kihelkonna Bay and NW Gulf of Riga, Soela Strait; Cluster 4: Pärnu and Matsalu Bay; Cluster 5: Eru-Käsmu, Hara and Kolga, central Gulf of Riga, Muuga-Tallinna-Kakumäe, Narva-Kunda, Pakri bays; Cluster 6: NE Gulf of Riga.

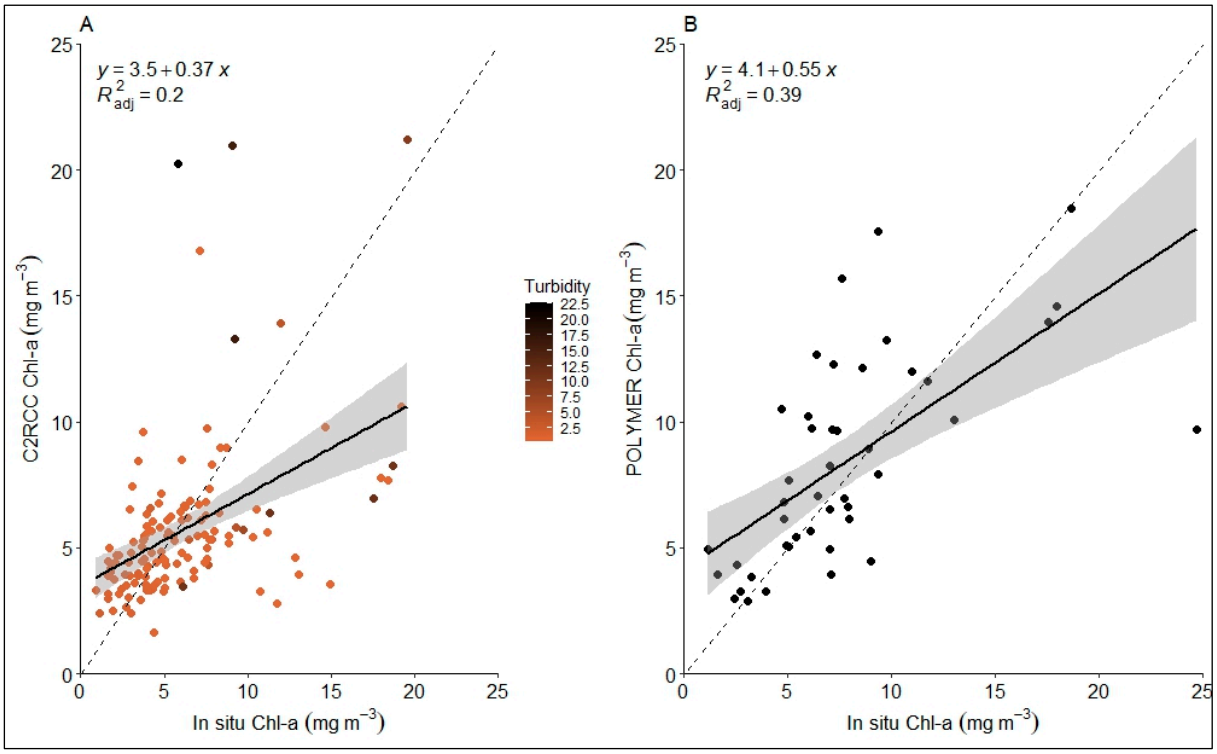

Figure 6. Scatterplot showing matchups between in situ chl-a (mg m^{-3}) and (**A**) C2RCC chl-a, (**B**) POLYMER chl-a. The satellite-derived turbidity (FNU) at sampling stations is given as a color-scale for C2RCC. The dashed line represents a 1:1 relationship, black line represents the line of best fit, and 95% confidence interval shown in grey.

3.1.2. N_2-Fixing Cyanobacterial Biomass

The N_2-fixing cyanobacteria are most prevalent during the summer in the Baltic Sea. As the name suggests, they fix nitrogen from the atmosphere and make nitrogen bioavailable which can have cascading effects on food webs [59,60]. The equation used here to estimate the biomass from the satellite data is based on a relationship between the MCI values against the in situ-measured N_2-fixing cyanobacteria biomass (mg m^{-3}):

$$\text{Biomass} = 346.33 \times \text{MCI}^2 + 1043.2 \times \text{MCI} + 1089.1 \quad (4)$$

The relationship between the in situ biomass and the MCI was relatively poor (R^2 = 0.39, $p < 0.05$). An important aspect is that the MCI method for estimating cyanobacteria biomass is only useful at higher concentrations (>300 mg m^{-3}). The MCI uses the red and NIR wavelengths that are also influenced by turbidity which makes it difficult to estimate low chl-a. The poor relationship here is partly explained by the very low concentrations of chl-a and higher turbidity in the coastal areas compared to inland lakes, where the MCI has previously been successfully used [61].

Monitoring the seasonality of cyanobacteria blooms is of key importance. Using satellites gives a better overview than only relying on in situ sampling for monitoring seasonality. The average in situ biomass was highest in the Hara and Kolga bays (731.4 mg m^{-3}) and Muuga-Tallinna-Kakumäe Bay (615.9 mg m^{-3}) and lowest in the Gulf of Riga (NW) (1.0 mg m^{-3}) and Moonsund Sea (1.3 mg m^{-3}). It is important to note that in situ measurements are point measurements and satellite data are an average of a polygon (black dots and line in Figure 7) or a 3 × 3 pixel (red stars in Figure 7). As can be seen from Figure 8 and especially from Figure 7, the in situ measurements are sparse both in time and space, only having measurements throughout the entire time series for four coastal areas. Additionally, the concurrence of satellite-derived biomass with data from in situ sampling points in Haapsalu Bay (Figure 7A) shows that satellite data can provide good coincidence with the in situ-measured values within one vegetation period. Many of the peaks of N_2-fixing cyanobacteria biomass would be missed when relying exclusively on in situ sampling. However, the in situ dataset considers all concentrations, whereas satellite data do not consider concentrations below 300 mg m^{-3}. In some of the coastal water bodies, in situ and satellite-derived biomass are relatively similar, mostly in the areas belonging to the Gulf of Finland. Most similar were the results in Soela Strait. On longer timescales (2016–2022), the largest differences between the two methods can be observed in the Haapsalu, Matsalu, and Pärnu bays (Figure 8). Although the averaged results for the years are similar, significant seasonal differences can be observed, for example, in Muuga-Tallinna-Kakumäe Bay, when comparing cyanobacteria biomass (Figures 7B and 8).

3.2. Indices for Phytoplankton Bloom Characterization

3.2.1. Phytoplankton Intensity Index (PII)

The Phytoplankton Intensity Index is a non-normalized index that is solely based on chl-a. Higher values correspond to more extensive blooms. Here, the PII values ranged from 0 to 1256 (Figure 8). Nine bays had a PII value of 0 during the time period under study. There is considerable variation between the index values in different years. The highest mean values were calculated for Matsalu Bay (PII = 740), Haapsalu Bay (691), and Pärnu Bay (619). Similarly, the highest values were estimated in Haapsalu Bay (1256), Matsalu Bay (1171), and Pärnu Bay (807) (Figure 9). It is likely that due to the nature of the bays, the results indicate phytoplankton blooms in the areas but not necessarily cyanobacterial biomass.

3.2.2. CSA Index

The CSA Index inputs include the chl-a and turbidity derived from satellite data. CSA Index values of 1 correspond to negligible to no-bloom events, whereas a value of 0 indicates extensive growth. The most extensive blooms according to the CSA Index (corresponding to the lowest CSA Index values) were in the Hara and Kolga bays, Kihelkonna Bay, and Moonsund Sea, where the index was 0 (Figure 9). The Hara and Kolga and Kihelkonna bays are very open coastal areas and are highly influenced by the rest of the Baltic Sea, whereas Moonsund Sea is a shallow coastal area between the large western islands and the Estonian west coast. Conversely, three coastal areas had years when there were no blooms (corresponding to a CSA Index of 1). These were Eru-Käsmu Bay, Kassari-Õunaku Bay, and Matsalu Bay. For CSA, considerable variation in the results was observed between different years, and extreme values were calculated for the bays in different years. Looking at the whole period (2016–2022), the median CSA Index was highest in Kassari-Õunaku Bay (CSA = 0.76), Moonsund Sea (0.71), and the Hara and Kolga bays (0.65), whereas the lowest values were calculated for Pärnu Bay (0.27), Narva-Kunda Bay (0.28), and the central Gulf of Riga (0.34) (Figure 9). The adjacent Kassari-Õunaku Bay and Moonsund Sea form an area between the large western islands and the mainland which could explain the similarities of the results. The Narva-Kunda and Pärnu bays and the central Gulf of Riga are all highly productive and nutrient-rich areas, and the three areas are all heavily influenced by river inflows. The two other parts of the Gulf of Riga (NW and NE) also showed low index values indicating high levels of water exchange between them.

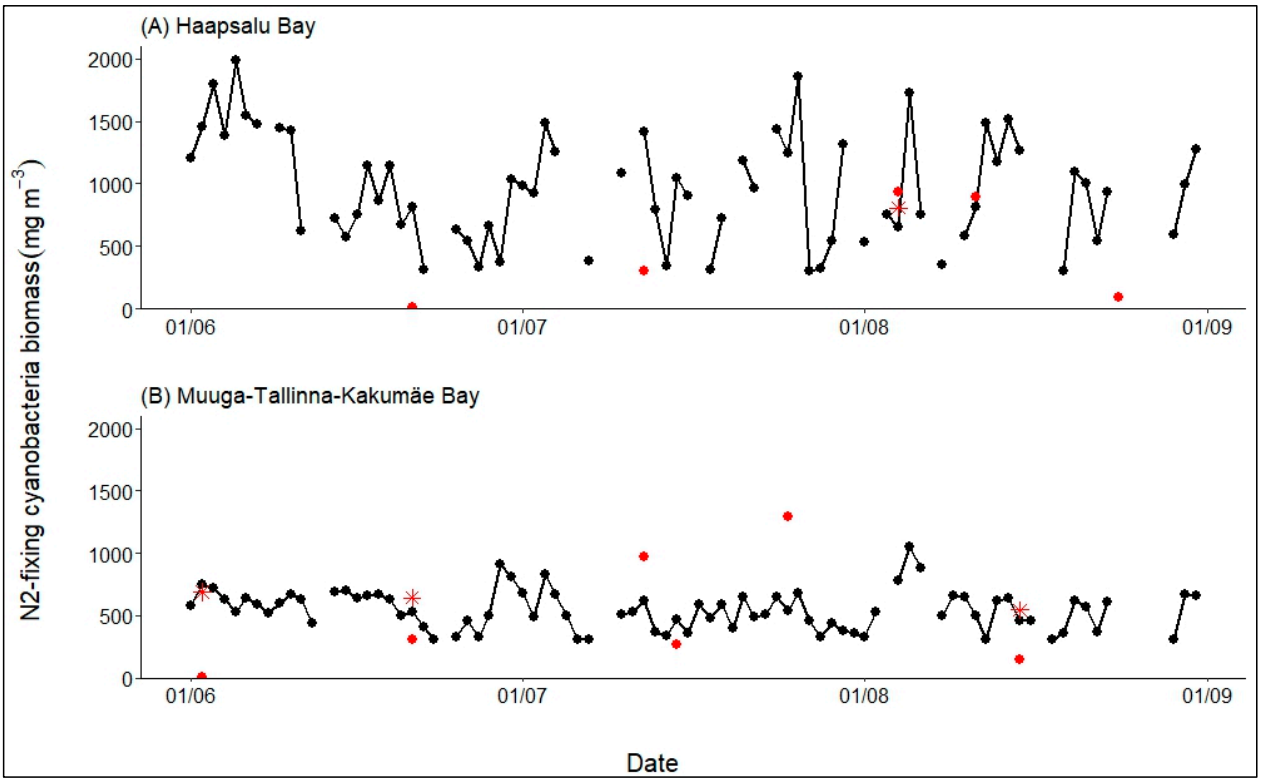

Figure 7. N_2-fixing cyanobacteria biomass (mg m^{-3}) in (**A**) Haapsalu Bay in 2021 and (**B**) Muuga-Tallinna-Kakumäe Bay in 2022 from June to September estimated from OLCI (polygon average, black dots and line), from in situ samples (average of the sampling station measurements, red dots) and satellite-derived values from station locations (red stars).

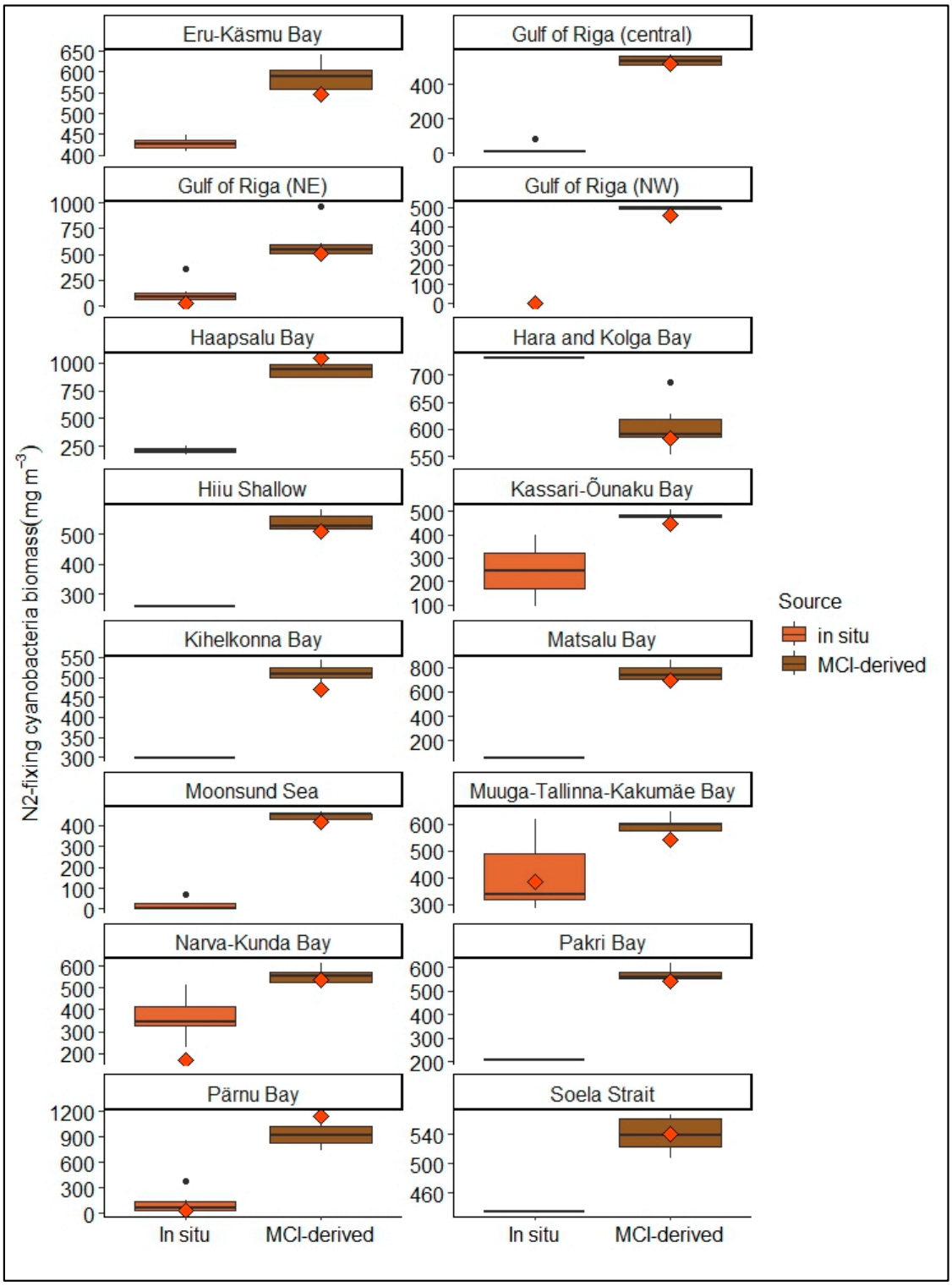

Figure 8. In situ (station average) and satellite-derived (polygon average) N_2-fixing cyanobacterial biomass (mg m^{-3}) in the years 2016–2022 in Estonian coastal areas. Boxplots represent 2016–2021 values (boxes represent IQR, middle line represents median, whiskers represent maximum and minimum values, and black dots represent outliers), and orange-red diamonds represent 2022 values. Note the scale differences in the *y*-axis.

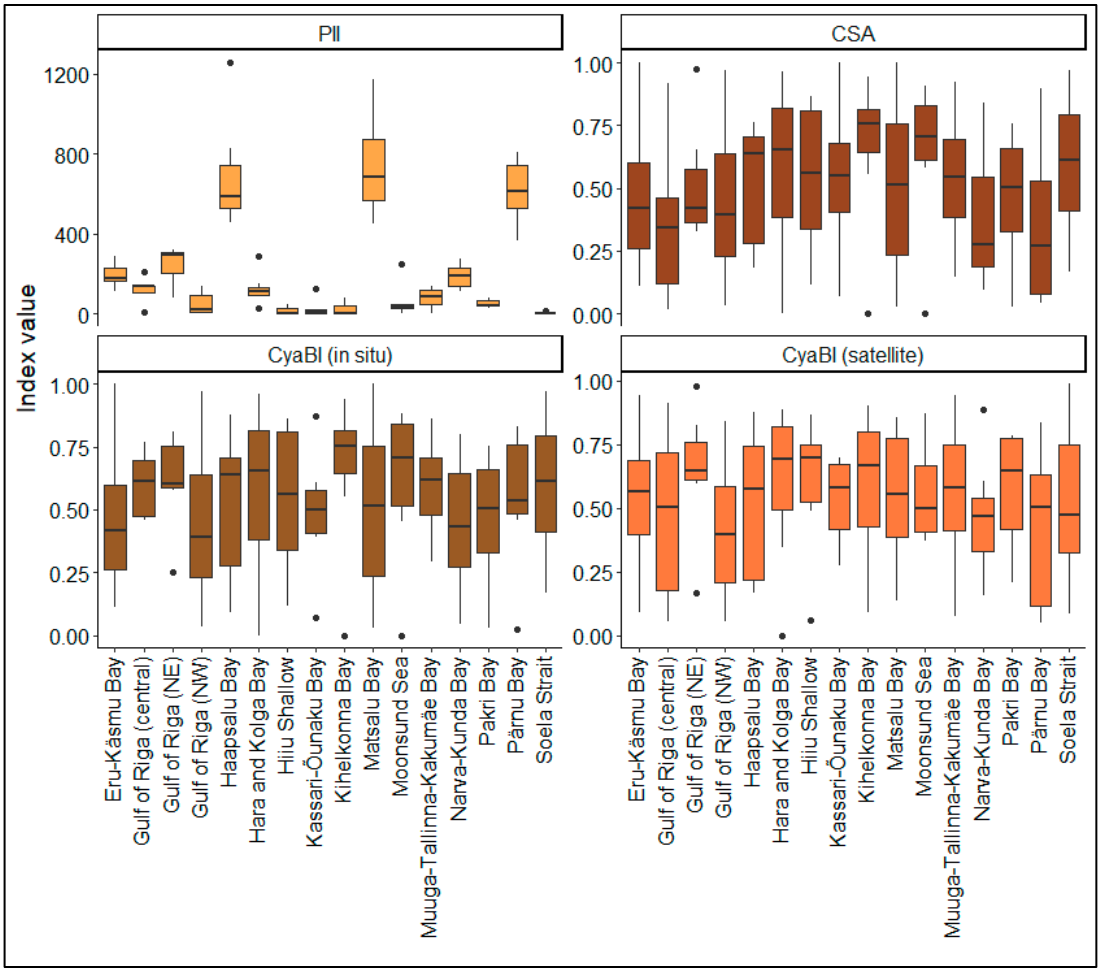

Figure 9. PII, CSA, in situ CyaBI, and satellite-derived CyaBI indices in Estonian coastal areas. Boxes represent the IQR of index values, the middle line represents the median, the whiskers represent the minimum and maximum values, and black dots represent outliers.

3.2.3. CyaBI with In Situ Cyanobacterial Biomass

Similar to the CSA Index, the CyaBI indicator values of 1 correspond to negligible to no-bloom events, whereas a value of 0 indicates extensive blooms. The inputs for the CyaBI include satellite-derived chl-a and turbidity as well as in situ N_2-cyanobacteria biomass. The most substantial blooms according to the CyaBI with in situ cyanobacterial biomass (corresponding to the lowest indicator values) were in the Hara and Kolga bays, Kihelkonna Bay, and Moonsund Sea (CyaBI = 0) (Figure 9). These results are similar to the CSA results, as is expected because the Hara and Kolga bays and Moonsund Sea had very limited in situ biomass data. Considerable variation in the results was observed between the different years, and extreme values were calculated for the bays in different years. The highest indicator values were calculated for Eru-Käsmu Bay, Matsalu Bay (CyaBI = 1), and the NW Gulf of Riga (0.97). For the whole period (2016–2022), the median CyaBI was highest in Kihelkonna Bay (0.76), Moonsund Sea (0.71), and the Hara and Kolga bays (0.65). The lowest median CyaBI values were calculated for Liivi Bay (NW) (0.39), Eru-Käsmu Bay (0.42), and Narva-Kunda Bay (0.43) (Figure 9). Narva-Kunda and Eru-Käsmu lie on the Northern coast, in the Gulf of Finland, and are heavily influenced by waves and river inputs. The three bays with the lowest values had a lot of available in situ cyanobacteria biomass data. The cyanobacteria biomass parameter gives an indication of the actual biomass in the water column and thus supplements the surface measurements of the RS data, giving more reliable results. Different results for these three bays between CSA and the CyaBI indicate a benefit of the addition of a

biomass parameter into the status assessments. Similar to the CSA, all three water bodies in the Gulf of Riga had relatively low values of the CyaBI (in situ).

3.2.4. CyaBI with Satellite-Derived Cyanobacterial Biomass

The inputs used for the CyaBI (satellite) included satellite-derived chl-a, turbidity, and N_2-fixing cyanobacteria biomass. The most extensive blooms according to the CyaBI with satellite-derived cyanobacterial biomass (corresponding to the lowest indicator values) were in the Hara and Kolga bays (CyaBI = 0), Pärnu Bay (0.05), and the NW Gulf of Riga (0.05) (Figure 9). The highest indicator values were calculated for Soela Strait (0.99), the NE Gulf of Riga (0.98), and Muuga-Tallinna-Kakumäe Bay (0.94). Like in the case of other indices, considerable variation in the results was observed between different years for the CyaBI (satellite), and extreme values were calculated for the bays in different years. For the whole period (2016–2022), the median CyaBI was highest in Hiiu Shallow (0.70), the Hara and Kolga bays (0.69), and Kihelkonna Bay (0.67). All three of the coastal areas are open to the larger Baltic Sea. The lowest median CyaBI values were calculated for the NW Gulf of Riga (0.39), Narva-Kunda Bay (0.47), and Soela Strait (0.47) (Figure 9). The satellite CyaBI showed the largest contrast to the rest of the indices. Although the two areas neighbor each other on the west coasts of Saaremaa and Hiiumaa, Soela Strait had one of the lowest index values, whereas Kihelkonna Bay had the highest. Unlike the CyaBI (in situ) and CSA, only one of the Gulf of Riga water bodies had a very low index value. In contrast to previous indices, the variation within the whole Gulf of Riga according to the CyaBI (satellite) was very high.

3.3. Current Environmental Status of Estonian Coastal Areas

Taking the 75th percentile of the results in the years 2016–2021 gave the threshold value for deciding whether GES is reached in a coastal area in 2022. The results showed a lot of variation from area to area. The NW Gulf of Riga achieved a GES according to all four indices; however, the threshold values there were much lower than in other areas (PII = 105, CSA = 0.55, CyaBI (in situ) = 0.55, and CyaBI (satellite) = 0.49) (Table 4) and the results are exclusively reliant on satellite-derived data as the NW Gulf of Riga did not have in situ sampling stations before 2022. Out of 16 coastal areas, 5 did not reach GES under any of the four methodologies—the Haapsalu, Hara and Kolga, NE Gulf of Riga, Matsalu, and Pärnu bays. Another seven areas reached GES according to only one index. Reaching GES was most difficult according to the CSA Index, under which only the NW Gulf of Riga achieved it (Appendix A, Figure A1).

Table 4. Environmental status of the coastal areas in 2022 compared to threshold values for the 4 indices. Results underlined and in bold represent reaching GES.

Coastal Area	CSA Index		CyaBI (In Situ)		CyaBI (Satellite)		Phytoplankton Intensity Index	
	Threshold	2022	Threshold	2022	Threshold	2022	Threshold	2022
Eru-Käsmu Bay	0.67	0.34	0.67	0.34	0.67	0.66	237	**173**
Haapsalu Bay	0.73	0.33	0.73	0.33	0.78	0.17	633	1256
Hara and Kolga bays	0.84	0.52	0.84	0.52	0.83	0.64	112	148
Hiiu Shallow	0.82	0.13	0.82	0.13	0.75	0.56	28	**15**
Kassari-Õunaku Bay	0.71	0.39	0.59	0.39	0.64	**0.69**	16	16
Kihelkonna Bay	0.81	0.80	0.81	0.80	0.76	**0.90**	59	**0**
Gulf of Riga (center)	0.47	0.16	0.71	0.61	0.73	0.51	142	**135**
Gulf of Riga (NE)	0.61	0.42	0.75	0.71	0.78	0.69	304	312
Gulf of Riga (NW)	0.55	**0.68**	0.55	**0.68**	0.49	**0.84**	105	**0**
Matsalu Bay	0.79	0.03	0.79	0.03	0.80	0.43	813	1171
Muuga-Tallinna-Kakumäe Bay	0.71	0.54	0.73	0.62	0.69	**0.77**	123	**47**
Narva-Kunda Bay	0.66	0.28	0.60	**0.64**	0.57	0.47	237	**155**
Pakri bays	0.67	0.21	0.67	0.21	0.77	0.60	71	**42**
Pärnu Bay	0.60	0.04	0.79	0.51	0.64	0.05	670	794
Soela Strait	0.85	0.27	0.85	0.27	0.79	0.36	0 *	0 *
Moonsund Sea	0.86	0.00	0.86	0.00	0.71	0.50	46	**27**

* Chl-a did not exceed 5 mg m^{-3} in Soela Strait.

4. Discussion

Monitoring and managing aquatic resources is necessary to ensure the safety of marine environments. The MSFD sets out rules for all European member states to organize efforts to monitor and improve their coastal areas. Under the MSFD, Estonian coastal waters need to be monitored and GES must be reached and maintained [24]. The formation of HABs by cyanobacteria is a parameter for estimating the ES of an area and is one part of the larger monitoring scheme for the MSFD and the national environmental monitoring scheme in Estonian waters [62,63]. The purpose of the assessment is to obtain the current status of the Estonian coastal areas as input for improving the conditions of the areas—where to focus adaptation and remediation efforts. The use of satellite data in the assessment could be of benefit to monitoring programs as a quicker and more extensive tool for the short- to long-term monitoring of coastal waters. An additional benefit of satellite data to the public is the quicker availability and spatial coverage of information about HABs in contrast to in situ sampling.

The first goal of this study was to assess the applicability of the C2RCC and POLYMER processors, which have previously shown good results in regions influenced by high phytoplankton biomass (high chl-a), CDOM, and TSM [56,64–66]. C2RCC has been shown to be useful in many different water bodies, for example, in the Baltic Sea [47] or in Estonian and Latvian lakes [67]. However, the Baltic Sea is an optically complex water body, where atmospheric correction and bio-optical modeling are difficult as evidenced by previous results by Toming et al. [57] and Kratzer and Plowey [56] in coastal areas in the Baltic Sea, where chl-a is typically lower and where influence by CDOM is high [47,68]. Nonetheless, C2RCC and POLYMER have previously shown the most promise for chl-a detection which was the reason for their selection here. Our validation of the two satellite data processors provided rather poor match-ups with the in situ chl-a (Figure 6). Our data also showed that very high chl-a (>20 mg m^{-3}) estimated by C2RCC was often highly turbid (>15 FNU) with low corresponding in situ chl-a (<10 mg m^{-3}) (Figure 6). This makes it difficult to accurately estimate chl-a in highly turbid areas, like the Pärnu, Matsalu, or Haapsalu bays. Similar to Kyryliuk et al. [47], C2RCC tended to underestimate high chl-a at points where the turbidity was low (<5 FNU) (Figure 6). Although the POLYMER validation provided a higher coefficient of determination (R^2 = 0.39), the processor flags significantly more pixels. This is an issue when the goal of using satellite data for an environmental status assessment is to cover an area of interest as frequently as possible. One reason for the poor results received from our validation analysis is the difference in the collection methodology of chl-a. The satellite data consist of pixels covering an area of 300 m × 300 m, whereas the in situ data consist of depth-integrated point measurements. The current way of gathering in situ samples is via ships which has previously been criticized as mixing the water column and disrupting the surface bloom, providing results that are not in accordance with the actual conditions [20]. Additionally, the current methodology aggregates chl-a from depths of 0–10 m below sea level which is an issue in cases where prevalent surface and subsurface blooms or turbidity of the water hinder light penetration to those depths. *Nodularia spumigena*, for example, forms dense surface blooms [31]. In order to improve the accuracy of chl-a detection, advances in bio-optical modeling and the use of hyperspectral sensors could be future research areas.

Comparing N_2-fixing cyanobacteria biomass gathered in situ, it was observed that biomass from satellites tended to overestimate the actual biomass measured at sampling stations. It has been previously documented that the MCI works better with higher chl-a [51], whereas chl-a in Estonian coastal areas is relatively low with seasonal dynamics responsible for high peaks (IQR = 2.8–6.1 mg m^{-3}, median = 4.1 mg m^{-3}). However, the use of the MCI for determining cyanobacteria biomass from satellite data is likely to be the reason for high satellite-derived biomass values in the Pärnu, Matsalu, and Haapsalu bays, as high chl-a was present in these areas. Because the MCI is high when there are surface planktonic blooms or aquatic vegetation, it does not discriminate between groups of phytoplankton or other vegetation and has been used to monitor, e.g., *Sargassum* and algal blooms in the Baltic Sea and the Arctic [69,70]. Nonetheless, the MCI-derived values are best suited to compare different areas and to map potential bloom areas. Our

results showed that the dynamics of the blooms when the biomass is above 300 mg m^{-3} can be monitored. The differences between the in situ and EO data are a result of the differences in both methodologies. In situ sampling is more accurate at a singular point but does not give an overview of the entire area, whereas satellite-derived biomass covers a larger area but suffers from the inability to detect low biomass values in the presence of high CDOM (e.g., absorption at Pärnu Bay 1.38–14.08 m^{-1}) [40] and TSM (e.g., Pärnu Bay 5–24.3 g m^{-3}) [71]. In situ biomass sampling also suffers from the same drawbacks as the sampling of chl-a discussed above—besides more frequently monitored areas, there is a lack of consistent data for others. Even then, our cluster analysis has shown seasonal variability in the chl-a and turbidity which would have been missed without the satellites, adding to the usefulness of using EO data for monitoring. Regarding the difficulty of deriving biomass from satellite data, cyanobacteria are typically estimated in the form of an index [72]. Developing more accurate algorithms for the detection of cyanobacteria from satellites is necessary. Difficulties in assessing cyanobacteria from satellite data, especially in areas with low biomass, are not unique to the method used here but are known issues with current remote monitoring techniques as evidenced in [51,72–74].

The indices are largely based on satellite-derived chl-a with additional inputs from turbidity and cyanobacteria biomass. The CSA, CyaBI (in situ), and CyaBI (satellite) showed comparable results for the coastal areas (Figure 9). Chl-a is used as a proxy for all types of phytoplankton and aquatic vegetation biomass [28]. Because the PII is solely based on chl-a, it gives the least additional information about the presence of cyanobacteria biomass. The three species of cyanobacteria included in our analysis, *Aphanizomenon*, *Nodularia*, and *Dolichospermum*, did not correlate well with the in situ chl-a (the best result being *Aphanizomenon*, $R^2 = 0.15$, $p > 0.05$). As such, on its own, using the PII is the least useful for coastal areas, where other vegetation or a bloom event consisting of other species of phytoplankton are present. Other indices do not show significant differences in the results of the Haapsalu, Matsalu, and Pärnu bays and the rest of the coastal areas, whereas the PII does.

Originally, chl-a was intended to be used as a proxy for cyanobacterial biomass and turbidity was intended to indicate the presence of dead cyanobacteria cells in open sea areas [17]. In calculating the CSA Index, turbidity is used as an input to classify cyanobacteria blooms in pixels. In the case of Estonian coastal areas, not only is turbidity caused by organic material but is most likely dominated by mineral particles, especially in the case of shallow areas and strong wind events [75]. For this reason, in Estonian coastal areas, the CSA Index, like other indices, is limited in differentiating between cyanobacteria biomass and other phytoplankton. Additionally, the relationship between chl-a and turbidity is not linear in most coastal areas (Appendix B, Figure A2), and according to our cluster analysis, a peak in chl-a is not followed by peaks in turbidity as would be expected if dead cyanobacteria cells were present in the area after a chl-a peak. One exception is Haapsalu Bay, where a peak in chl-a is followed by higher turbidity (Figure 4 cluster 1, and Figure 5 cluster 2). However, the shallow parts of Haapsalu Bay are dominated by bottom vegetation covering parts of the sea which could also explain the high chl-a picked up by the satellite. Although supplementing turbidity and chl-a with cyanobacteria biomass would lead to more accurate estimates, in the absence of such data, the CSA Index could be used for Haapsalu Bay with consideration for possible bottom vegetation influence, especially in the late summer.

Estimating chl-a and turbidity from satellite data allows for spatial and temporal coverage not possible with in situ measurements. However, these parameters have deficiencies regarding the accurate estimation of cyanobacteria biomass [17,28]. Our results indicate a similar deficiency as areas with high chl-a and turbidity showed values indicative of cyanobacteria blooms under CSA and the PII but did not show high N_2-fixing cyanobacteria biomass. This resulted in more favorable CyaBI (both in situ and satellite) values in 2022 for the Pärnu, Muuga-Tallinna-Kakumäe, and Narva-Kunda bays and the NE Gulf of Riga compared to the CSA and PII values in those areas (Table 3). Because of this, the most applicable index is the CyaBI in coastal areas which are naturally turbid and have a lot of chl-a

(Pärnu, Matsalu, and Haapsalu bays). Both the satellite-derived and in situ CyaBI have their merits over the other. The use of the CyaBI (in situ) is most applicable in coastal areas where satellite-derived N_2-fixing biomass is the most difficult to assess, such as the Pärnu, Matsalu, and Haapsalu bays. These areas are dominated by CDOM and TSM. This index benefits from the use of both in situ cyanobacterial biomass and satellite-derived turbidity and chl-a. In situ measurements, however, are sparse, as evidenced in the frequency of the measurements in Table 1. It would be advisable to supplement the satellite-derived chl-a and turbidity estimates with in situ cyanobacteria biomass, but in areas where turbidity is less of a factor (<1 FNU), the use of satellite-derived biomass is possible e.g., the Hara and Kolga, Eru-Käsmu, or Muuga-Tallinna-Kakumäe bays, and would provide better temporal coverage. In such areas, the CyaBI (satellite) could be used.

An additional goal of this study was to assess the current ES in the Baltic Sea on the Estonian coast during the summer cyanobacteria bloom events from 2016 to 2022 using four indices that have previously been applied in the region. As mentioned in Section 3.3, there were five coastal regions that did not achieve GES in 2022 under any of the four methodologies used in this study. It is unlikely to be an accurate estimate of ES in terms of describing cyanobacteria blooms, but rather a possible reason for these results could be the spatial and hydrological effects dominating these coastal areas. The Haapsalu, Matsalu, and Pärnu bays are heavily influenced by river and wetland inputs and wave dynamics, which increase the turbidity of the bays [40,76–78]. Particularly during windy days, the shallowness of these areas leads to high concentrations of resuspended bottom sediment in the water column [40]. High turbidity from sediments rather than dead cyanobacteria cells is one possible explanation for not achieving GES in these areas. From our analysis, higher satellite-derived chl-a was more evident when the turbidity was also higher even though the corresponding in situ-sampled chl-a was not (Figure 6A, where turbidity > 20 FNU). It also highlights why using the PII in turbid areas is disadvantageous as turbidity can inhibit accurate chl-a estimation. In the case of Pärnu Bay, for example, the 2022 in situ samples did not show significant cyanobacteria biomass in the area, whereas the turbidity was high. This would indicate an erroneous ES assessment as the turbidity is not a result of dead cyanobacteria cells but rather inorganic matter being picked up by the satellite.

Upwelling is a possible cause for the seasonal dynamics in the Gulf of Finland (Hara–Kolga, Eru-Käsmu, Muuga-Tallinna-Kakumäe, and Pakri bays) and in the NE Gulf of Riga. Upwelling in the Gulf of Finland (northern coast of Estonia) is a regular occurrence that displaces the warm surface water with cold water from the bottom layer of the sea while increasing nutrients in the upper layers. Because cyanobacteria generally prefer warmer temperatures and are normally phosphorous-limited [15,79], upwelling has an effect in areas where it occurs. Due to the variability in upwelling events, which might be seasonal or one-off events, it is difficult to measure its effect on the annual ES of a coastal area. Upwelling can have a promoting effect on the formation of cyanobacteria blooms as it enriches the higher water levels with phosphorous [80,81]. Other evidence has shown that the upwelling process can temporarily displace cyanobacteria species and disrupt the structure of community composition [82], but the effect is only temporary as communities tend to return to compositions similar to those before an upwelling event shortly after [82]. Water temperature which can be measured via satellites can be used as an additional parameter for future ES assessments which would link the impacts of upwelling to the environmental status assessment.

An important aspect to note is the large year-to-year variation in the index results which shows high natural variability in the bloom parameters. Due to the limitations of using S3/OLCI data, our dataset extends only as far back as 2016. Because of this, the period from which a threshold ES value is calculated is rather small and might skew the result if an area has had a particularly turbid or chl-a-dominated year. The reliability of determining the "good-bad" threshold value and environmental status depends mainly on the representativeness of the data. Because the variability between years can be quite impressive, it would be beneficial to assess the environmental status of an area over a larger

time frame. On the other hand, the data series analyzed here cannot be extended into the very distant past due to differences in EO instruments. In general, however, the results indicating the poor environmental status of the coastal areas are consistent with other methodologies. Previous assessments by HELCOM [37] indicated a poor environmental status based on the CyaBI in the Gulf of Finland, Gulf of Riga, Eastern Gotland Basin, and Northern Baltic Proper (areas that include Estonian coastal areas). However, under HELCOM's methodology, no sampling took place in the NW part of the Gulf of Riga, which, according to our analysis, achieved GES. This highlights the usefulness as well as the necessity of using satellites for more accurate monitoring. Similar to HELCOM, a national monitoring report by the Estonian Environment Agency indicated a poor environmental status for some Estonian coastal areas (Gulf of Riga (NW), Gulf of Riga (center), Pärnu Bay, Muuga-Tallinna-Kakumäe Bay, and Narva-Kunda Bay). Their assessment methodology is based on other factors instead of cyanobacteria blooms, such as plankton, bottom vegetation, and bottom fauna [83]. As the Sentinel-3 mission is going to continue [49], a longer time period for threshold detection would be beneficial.

Future work should also focus on connecting the ES results as well as the chl-a given here to other environmental variables to explain the possible causes of the conditions of coastal areas. Causes will most likely differ between coastal areas. Some possible reasons for the results could be connected to temperature and nutrient inputs to the coastal areas via coastal upwelling [80] or inputs from rivers which might explain differences between coastal water bodies. Increases in atmospheric and aquatic CO_2 could also have a promoting effect on blooms but would influence all coastal areas comparably [9,84]. To further improve the indices for cyanobacteria monitoring, another pigment showing promising results, phycocyanin (PC) [85–87], could be added to the assessment. As PC detection improves, future work could include a measure of PC to better differentiate between cyanobacteria and other phytoplankton.

5. Conclusions

Cyanobacterial blooms are a nuisance to ecosystems, aquaculture, and public health. Thus, monitoring bloom parameters is of importance to society at large. Under the MSFD, European waters, including the Baltic Sea, must reach and maintain GES. Using satellite remote sensing for monitoring purposes could be a useful way to fill any gaps in the data and supplement the monitoring process. The impacts of climate change on the cyanobacteria communities will vary geographically and no single solution is applicable to all [84,88,89]. Here, we show four different approaches to assessing the ES of Estonian coastal areas based on satellite-derived chl-a, turbidity, and cyanobacterial biomass estimates. Satellite data allow for spatial and temporal resolution which in situ measurements cannot match. However, in situ sampling provides the necessary validation and can be useful for tuning the algorithms and developing new RS-based methods. Different approaches to assessing coastal areas are recommended as the areas differ from each other regarding chl-a, turbidity, and N_2-fixing cyanobacteria biomass. However, overall, the CyaBI gives the most comprehensive assessment of cyanobacteria blooms, with the satellite-derived CyaBI being better suited in large areas which would be difficult to accurately cover with in situ sampling and which are less impacted by CDOM and TSM. The CSA index could be useful in Haapsalu Bay in the absence of in situ cyanobacteria biomass data, where a peak in chl-a is followed by a slight increase in turbidity. We have presented threshold values for all 16 coastal areas and four indices to be used in assessments. As new data emerge, threshold values can be updated to reflect the environmental status better. Comparing the 2022 index results to the threshold values, it was found that most coastal areas failed to achieve GES under one or multiple indices. The NW Gulf of Riga was the only area where GES was achieved according to all four indices. Five areas, mostly closed bays, did not achieve GES under any of the four indices. We have also discussed the current limitations and inaccuracies associated with using satellite data in Case-2 coastal waters. Research into improving the current processors needs to be undertaken, especially in complex areas

which are heavily influenced by various environmental parameters. Assessing bloom parameters with satellite data could complement in situ monitoring practices with the provision of a more frequent and spatially expansive overview.

Author Contributions: Conceptualization, I.-A.R., K.K. and K.A.; Methodology, I.-A.R., K.K. and K.A.; Resources, K.K., K.A. and A.J.; Validation, I.-A.R., K.K. and K.A.; Formal analysis, I.-A.R.; Investigation, I.-A.R.; Data curation, I.-A.R., K.K., K.A. and A.J.; Writing—original draft preparation, I.-A.R.; Writing—review and editing, K.K., K.A. and A.J.; Supervision, K.K. and K.A.; Visualization, I.-A.R.; Project administration, K.K. and K.A.; Funding acquisition, K.K. and K.A. All authors have read and agreed to the published version of the manuscript.

Funding: This research was funded by the Estonian Environmental Agency, under the project "Further development of evaluation indicators of criterion D5C3 in accordance with the EU Marine Strategy Framework Directive (2008/56/EC) for specifying assessments of the state of the Estonian coastal area", and by the European Commission project No. FPA 275/G/GRO/COPE/17/10042, FPCUP (Framework Partnership Agreement on Copernicus User Uptake) action 2020-3-24 (Open Data Framework in the Baltic Sea Catchment Area).

Data Availability Statement: Data are available upon request, [link KESE].

Acknowledgments: We thank the ESA for the availability of the Sentinel 3/OLCI data, the Estonian Marine Institute for the in situ monitoring data, the Estonian Environmental Agency for the temperature data, and the Estonian Land Board for the availability of the processing environment ESTHub. We would also like to thank the three anonymous reviewers for their comments and ideas for improving the article.

Conflicts of Interest: The authors declare no conflict of interest.

Appendix A

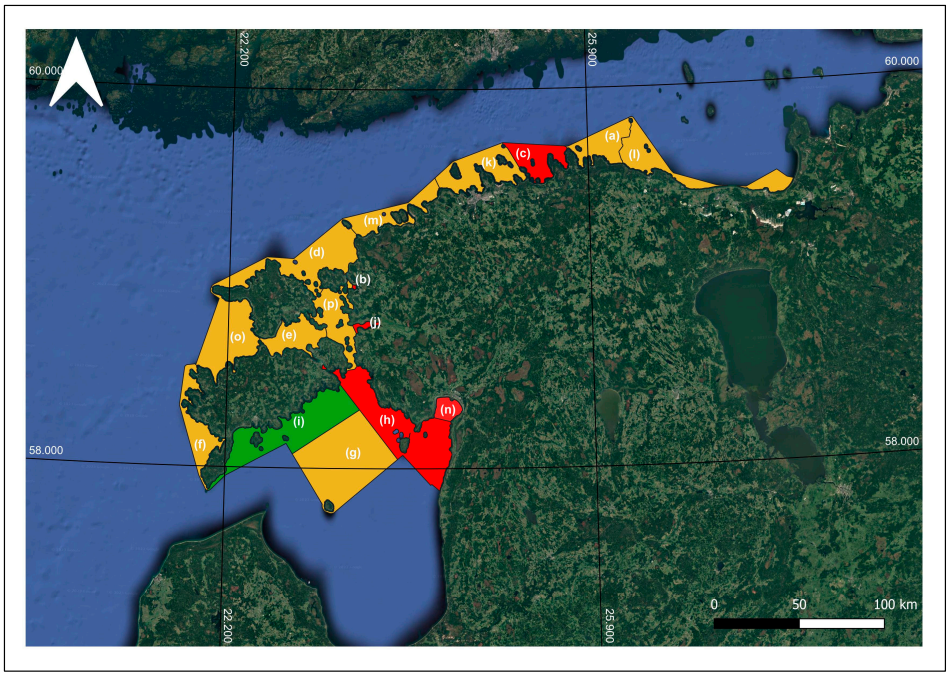

Figure A1. The results of the ES assessment in 2022 for all Estonian coastal areas. In green: area achieved GES according to all 4 indices; in yellow: area achieved GES according to some but not all indices; in red: areas failed to achieve GES according to any of the indices. (a) Eru-Käsmu Bay, (b) Haapsalu Bay, (c) Hara and Kolga bays, (d) Hiiu Shallow, (e) Kassari-Õunaku Bay, (f) Kihelkonna Bay, (g) Central Gulf of Riga, (h) NE Gulf of Riga, (i) NW Gulf of Riga, (j) Matsalu Bay, (k) Muuga-Tallinna-Kakumäe Bay, (l) Narva-Kunda Bay, (m) Pakri bays, (n) Pärnu Bay, (o) Soela Strait, (p) Moonsund Sea. Base image: Google Hybrid.

Appendix B

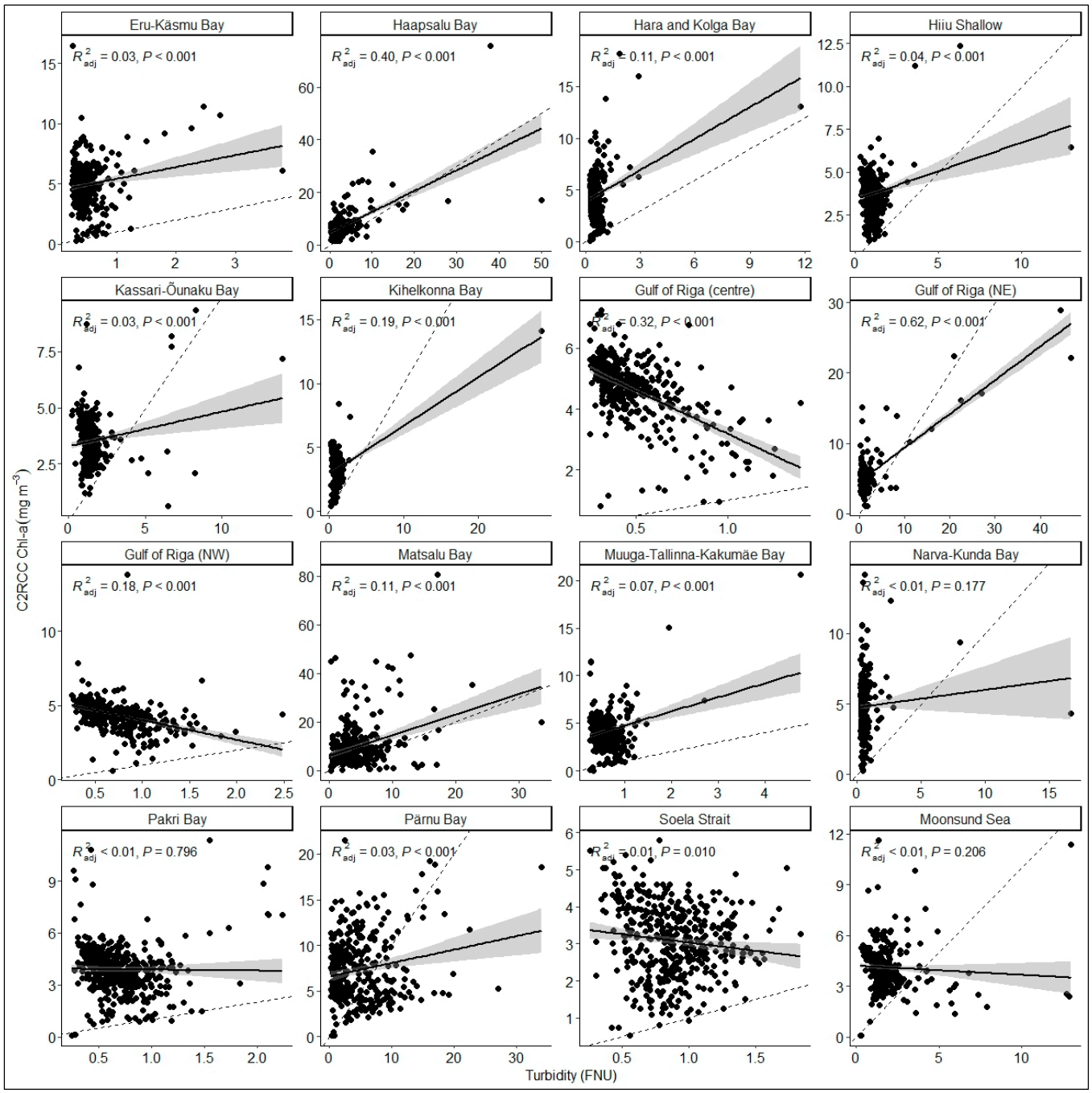

Figure A2. Relationship between satellite-derived chl-a and turbidity for each coastal area. The dashed line represents a 1:1 relationship, black line represents the line of best fit, and 95% confidence interval is shown in grey.

References

1. HELCOM. Thematic Assessment of Eutrophication 2011–2016. Baltic Sea Environment Proceedings No. 156. 2018. Available online: www.helcom.fi/baltic-sea-trends/holistic-assessments/state-of-the-baltic-sea-2018/reports-and-materials/ (accessed on 7 May 2023).
2. Andersen, J.H.; Axe, P.; Backer, H.; Carstensen, J.; Claussen, U.; Fleming-Lehtinen, V.; Järvinen, M.; Kaartokallio, H.; Knuuttila, S.; Korpinen, S.; et al. Getting the measure of eutrophication in the Baltic Sea: Towards improved assessment principles and methods. *Biogeochemistry* **2011**, *106*, 137–156. [CrossRef]
3. Suikkanen, S.; Pulina, S.; Engström-Öst, J.; Lehtiniemi, M.; Lehtinen, S.; Brutemark, A. Climate Change and Eutrophication Induced Shifts in Northern Summer Plankton Communities. *PLoS ONE* **2013**, *8*, e66475. [CrossRef]

4. HELCOM. Thematic Assessment of Eutrophication 2011–2016. Baltic Sea Environment Proceedings No. 155. 2018. Available online: http://www.helcom.fi/baltic-sea-trends/holistic-assessments/state-of-the-baltic-sea-2018/ (accessed on 8 May 2023).
5. Löptien, U.; Dietze, H. Retracing cyanobacteria blooms in the Baltic Sea. *Sci. Rep.* **2022**, *12*, 10873. [CrossRef]
6. Karlson, B.; Arneborg, L.; Johansson, J.; Linders, J.; Liu, Y.; Olofsson, M. A suggested climate service for cyanobacteria blooms in the Baltic Sea–Comparing three monitoring methods. *Harmful Algae* **2022**, *118*, 102291. [CrossRef] [PubMed]
7. Huisman, J.; Codd, G.A.; Paerl, H.W.; Ibelings, B.W.; Verspagen, J.M.H.; Visser, P.M. Cyanobacterial blooms. *Nat. Rev. Microbiol.* **2018**, *16*, 471–483. [CrossRef] [PubMed]
8. Kahru, M.; Elmgren, R. Multidecadal time series of satellite-detected accumulations of cyanobacteria in the Baltic Sea. *Biogeosciences* **2014**, *11*, 3619–3633. [CrossRef]
9. Taranu, Z.E.; Gregory-Eaves, I.; Leavitt, P.R.; Bunting, L.; Buchaca, T.; Catalan, J.; Domaizon, I.; Guilizzoni, P.; Lami, A.; McGowan, S.; et al. Acceleration of cyanobacterial dominance in north temperate-subarctic lakes during the Anthropocene. *Ecol. Lett.* **2015**, *18*, 375–384. [CrossRef]
10. Anderson, D.M. Approaches to monitoring, control and management of harmful algal blooms (HABs). *Ocean. Coast. Manag.* **2009**, *52*, 342–347. [CrossRef]
11. Carmichael, W.W. Health effects of toxin-producing cyanobacteria: 'The CyanoHABs'. *Hum. Ecol. Risk Assess.* **2001**, *7*, 1393–1407. [CrossRef]
12. Grattan, L.M.; Holobaugh, S.; Morris, J.G. Harmful algal blooms and public health. *Harmful Algae* **2016**, *57*, 2–8. [CrossRef] [PubMed]
13. Chorus, I.; Welker, M. Toxic Cyanobacteria in Water. In *A Guide to Their Public Health Consequences, Monitoring and Management*, 2nd ed.; CRC Press: Boca Raton, FL, USA, 2021. [CrossRef]
14. Bianchi, T.S.; Engelhaupt, E.; Westman, P.; Andrén, T.; Rolff, C.; Elmgren, R. Cyanobacterial blooms in the Baltic Sea: Natural or human-induced? *Am. Soc. Limnol. Oceanogr.* **2000**, *45*, 716–726. [CrossRef]
15. Munkes, B.; Löptien, U.; Dietze, H. Cyanobacteria blooms in the Baltic Sea: A review of models and facts. *Biogeosciences* **2021**, *18*, 2347–2378. [CrossRef]
16. Reinart, A.; Kutser, T. Comparison of different satellite sensors in detecting cyanobacterial bloom events in the Baltic Sea. *Remote Sens. Environ.* **2006**, *102*, 74–85. [CrossRef]
17. Anttila, S.; Attila, J.; Junttila, S.; Alasalmi, H. A novel earth observation based ecological indicator for cyanobacterial blooms. *Int. J. Appl. Earth Obs. Geoinf.* **2018**, *64*, 145–155. [CrossRef]
18. Bresciani, M.; Giardino, C.; Rosaria, L.; Matta, E. Earth observation for monitoring and mapping of cyanobacteria blooms. Case studies on five Italian lakes. *J. Limnol.* **2017**, *76*, 127–139. [CrossRef]
19. Reynolds, N.; Schaeffer, B.A.; Guertault, L.; Nelson, N.G. Satellite and in situ cyanobacteria monitoring: Understanding the impact of monitoring frequency on management decisions. *J. Hydrol.* **2023**, *619*, 129278. [CrossRef]
20. Kutser, T. Quantitative detection of chlorophyll in cyanobacterial blooms by satellite remote sensing. *Limnol. Oceanogr.* **2004**, *49*, 2179–2189. [CrossRef]
21. Cook, K.V.; Beyer, J.E.; Xiao, X.; Hambright, K.D. Ground-based remote sensing provides alternative to satellites for monitoring cyanobacteria in small lakes. *Water Res.* **2023**, *242*, 120076. [CrossRef]
22. Stumpf, R.P.; Davis, T.W.; Wynne, T.T.; Graham, J.L.; Loftin, K.A.; Johengen, T.H.; Gossiaux, D.; Palladino, D.; Burtner, A. Challenges for mapping cyanotoxin patterns from remote sensing of cyanobacteria. *Harmful Algae* **2016**, *54*, 160–173. [CrossRef]
23. Handler, A.M.; Compton, J.E.; Hill, R.A.; Leibowitz, S.G.; Schaeffer, B.A. Identifying lakes at risk of toxic cyanobacterial blooms using satellite imagery and field surveys across the United States. *Sci. Total Environ.* **2023**, *869*, 161784. [CrossRef]
24. European Union. Directive 2000/60/EC of the European Parliament and of the Council of 23 October 2000 Establishing a Framework for Community Action in the Field of Water Policy. Official Journal L 327, 22 December 2000, pp. 1–72. For Consolidated Version 2000L0060. 2014, pp. 1–93. Available online: https://eur-lex.europa.eu/legal-content/EN/TXT/?uri=CELEX%3A32000L0060 (accessed on 15 July 2023).
25. UN DESA. The Sustainable Development Goals Report 2022. UN DESA. 2022. Available online: https://unstats.un.org/sdgs/report/2022/ (accessed on 15 June 2023).
26. European Union. Directive 2008/56/EC of the European Parliament and of the Council of 17 June 2008 Establishing a Framework for Community Action in the Field of Marine Environmental Policy (Marine Strategy Framework Directive). Official Journal L 164, 25 June 2008. 2008, pp. 19–40. Available online: https://eur-lex.europa.eu/legal-content/EN/TXT/?uri=celex%3A32008L0056 (accessed on 15 July 2023).
27. Buelo, C.D.; Carpenter, S.R.; Pace, M.L. A modeling analysis of spatial statistical indicators of thresholds for algal blooms. *Limnol. Oceanogr. Lett.* **2018**, *3*, 384–392. [CrossRef]
28. Ferreira, J.G.; Andersen, J.H.; Borja, A.; Bricker, S.B.; Camp, J.; Cardoso da Silva, M.; Garces, E.; Heiskanen, A.-S.; Humborg, C.; Ignatiades, L.; et al. Overview of eutrophication indicators to assess environmental status within the European Marine Strategy Framework Directive. *Estuar. Coast. Shelf Sci.* **2011**, *93*, 117–131. [CrossRef]
29. HELCOM. Indicator Manual. Version 2020-1. Baltic Sea Environment Proceedings n°175. 2020. Available online: www.helcom.fi (accessed on 7 May 2023).
30. Fleming, V.; Kaitala, S. Phytoplankton spring bloom intensity index for the Baltic Sea estimated for the years 1992 to 2004. *Hydrobiologia* **2006**, *554*, 57–65. [CrossRef]

31. Kahru, M.; Elmgren, R.; Kaiser, J.; Wasmund, N.; Savchuk, O. Cyanobacterial blooms in the Baltic Sea: Correlations with environmental factors. *Harmful Algae* **2020**, *92*, 101739. [CrossRef] [PubMed]
32. Kahru, M.; Savchuk, O.P.; Elmgren, R. Satellite measurements of cyanobacterial bloom frequency in the Baltic Sea: Interannual and spatial variability. *Mar. Ecol. Prog. Ser.* **2007**, *343*, 15–23. [CrossRef]
33. Cazzaniga, I.; Zibordi, G.; Mélin, F. Spectral features of ocean colour radiometric products in the presence of cyanobacteria blooms in the Baltic Sea. *Remote Sens. Environ.* **2023**, *287*, 113464. [CrossRef]
34. Legleiter, C.J.; King, T.V.; Carpenter, K.D.; Hall, N.C.; Mumford, A.C.; Slonecker, T.; Graham, J.L.; Stengel, V.G.; Simon, N.; Rosen, B.H. Spectral mixture analysis for surveillance of harmful algal blooms (SMASH): A field-, laboratory-, and satellite-based approach to identifying cyanobacteria genera from remotely sensed data. *Remote Sens. Environ.* **2022**, *279*, 113089. [CrossRef]
35. Bunyon, C.L.; Fraser, B.T.; McQuaid, A.; Congalton, R.G. Using Imagery Collected by an Unmanned Aerial System to Monitor Cyanobacteria in New Hampshire, USA, Lakes. *Remote Sens.* **2023**, *15*, 2839. [CrossRef]
36. Choi, B.; Lee, J.; Park, B.; Sungjong, L. A study of cyanobacterial bloom monitoring using unmanned aerial vehicles, spectral indices, and image processing techniques. *Heliyon* **2023**, *9*, e16343. [CrossRef]
37. HELCOM. Cyanobacterial Bloom Index (CyaBI). 2018. Available online: https://helcom.fi/cyanobacterial-bloom-index-helcom-pre-core-indicator-2018-2/ (accessed on 27 November 2022).
38. Ministry of the Environment. 16 April 2020. A Määrus nr 19, Pinnaveekogumite Nimekiri, Pinnaveekogumite ja Territoriaalmere Seisundiklasside Määramise Kord, Pinnaveekogumite Ökoloogiliste Seisundiklasside Kvaliteedinäitajate Väärtused ja Pinnaveekogumiga Hõlmamata Veekogude Kvaliteedinäitajate Väärtused, Lisa 2. Last Revised 24 April 2020. Available online: https://www.riigiteataja.ee/akt/121042020061 (accessed on 20 July 2023).
39. Ministry of the Environment. 16 April 2020. A Määrus nr 19, Pinnaveekogumite Nimekiri, Pinnaveekogumite ja Territoriaalmere Seisundiklasside Määramise Kord, Pinnaveekogumite Ökoloogiliste Seisundiklasside Kvaliteedinäitajate Väärtused ja Pinnaveekogumiga Hõlmamata Veekogude Kvaliteedinäitajate Väärtused, Lisa 1. Last Revised 24 April 2020. Available online: https://www.riigiteataja.ee/akt/121042020061 (accessed on 20 July 2023).
40. Uusõue, M.; Ligi, M.; Kutser, M.; Bourrin, F.; Uudeberg, K.; Kangro, K.; Paavel, B. Effects of different conditions on particle dynamics and properties in West-Estonian coastal areas. *Oceanologia* **2022**, *64*, 694–716. [CrossRef]
41. HELCOM. Guidelines for Monitoring of Phytoplankton Species Composition, Abundance and Biomass. HELCOM. 2021. Available online: https://helcom.fi/wp-content/uploads/2020/01/HELCOM-Guidelines-for-monitoring-of-phytoplankton-species-composition-abundance-and-biomass.pdf (accessed on 19 July 2023).
42. HELCOM. Guidelines for Monitoring of Chlorophyll a. HELCOM. Available online: https://helcom.fi/wp-content/uploads/2019/08/Guidelines-for-measuring-chlorophyll-a.pdf (accessed on 19 July 2023).
43. Steinmetz, F.; Deschamps, P.-Y.; Ramon, D. Atmospheric correction in presence of sun glint: Application to MERIS. *Opt. Soc. Am.* **2011**, *19*, 9783–9800. [CrossRef] [PubMed]
44. Brockmann, C.; Doerffer, R.; Peters, M.; Stelzer, K.; Embacher, S.; Ruescas, A. Evolution of the C2RCC neural network for sentinel 2 and 3 for the retrieval of ocean colour products in normal and extreme optically complex waters. *Living Planet Symp.* **2016**, *2016*, 740.
45. Schiller, H.; Doerffer, R. Neural network for emulation of an inverse model operational derivation of Case II water properties from MERIS data. *Int. J. Remote Sens.* **1999**, *20*, 1735–1746. [CrossRef]
46. EUMETSAT. Recommendations for Sentinel-3 OLCI Ocean Colour Product Validations in Comparison with In Situ Measurements-Matchup Protocols. 2022. Available online: http://www.eumetsat.int (accessed on 20 December 2022).
47. Kyryliuk, D.; Kratzer, S. Evaluation of sentinel-3A OLCI products derived using the case-2 regional coastcolour processor over the Baltic Sea. *Sensors* **2019**, *19*, 3609. [CrossRef] [PubMed]
48. Gower, J.; King, S.; Goncalves, P. Global monitoring of plankton blooms using MERIS MCI. *Int. J. Remote Sens.* **2008**, *29*, 6209–6216. [CrossRef]
49. Donlon, C.; Berruti, B.; Buongiorno, A.; Ferreira, M.-H.; Femenias, P.; Frerick, J.; Goryl, P.; Klein, U.; Laur, H.; Mavrocordatos, C.; et al. The Global Monitoring for Environment and Security (GMES) Sentinel-3 mission. *Remote Sens. Environ.* **2012**, *120*, 37–57. [CrossRef]
50. Zeng, C.; Binding, C.E. Consistent multi-mission measures of inland water algal bloom spatial extent using meris, modis and olci. *Remote Sens.* **2021**, *13*, 3349. [CrossRef]
51. Binding, C.E.; Greenberg, T.A.; Bukata, R.P. The MERIS Maximum Chlorophyll Index; its merits and limitations for inland water algal bloom monitoring. *J. Great Lakes Res.* **2013**, *39*, 100–107. [CrossRef]
52. Nõges, P. Uuring Peipsi Järve Füüsikalis-Keemiliste ja Fütoplanktoni Kvaliteedinäitajate Klassipiiride Täpsustamiseks. Eesti Vabariigi Keskkonnaministeeriumi ja Eesti Maaülikooli Vahel 2 September 2020 Sõlmitud Töövõtuleping nr 4-1/20/131. 2020. Available online: https://dspace.emu.ee/xmlui/bitstream/handle/10492/7630/Peipsi%20vrd%20kriteeriumite%20aruanne.pdf?sequence=1&isAllowed=y (accessed on 1 March 2023).
53. Mischke, U.; Carvalho, L.; McDonald, C.; Skjelbred, B.; Solheim, A.L.; Philips, G.; de Hoyos, C.; Borics, G.; Moe, J.; Pahissa, J. Deliverable D3.1-2: Report on Phytoplankton Bloom Metrics. 2009. Available online: https://nora.nerc.ac.uk/15913/1/N015913CR.pdf (accessed on 12 May 2023).
54. Boyer, J.N.; Kelble, C.R.; Ortner, P.B.; Rudnick, D.T. Phytoplankton bloom status: Chlorophyll a biomass as an indicator of water quality condition in the southern estuaries of Florida, USA. *Ecol. Indic.* **2009**, *9*, S56–S67. [CrossRef]

55. United States Environmental Protection Agency. Nutrient Criteria Technical Guidance Manual: Estuarine and Coastal Marine Waters. 2001. Available online: https://www.epa.gov/sites/default/files/2018-10/documents/nutrient-criteria-manual-estuarine-coastal.pdf (accessed on 20 July 2023).
56. Kratzer, S.; Plowey, M. Integrating mooring and ship-based data for improved validation of OLCI chlorophyll-a products in the Baltic Sea. *Int. J. Appl. Earth Obs. Geoinf.* **2021**, *94*, 102212. [CrossRef]
57. Toming, K.; Kutser, T.; Uiboupin, R.; Arikas, A.; Vahter, K.; Paavel, B. Mapping water quality parameters with Sentinel-3 Ocean and Land Colour Instrument imagery in the Baltic Sea. *Remote Sens.* **2017**, *9*, 1070. [CrossRef]
58. Soomets, T.; Toming, K.; Paavel, B.; Kutser, T. Evaluation of remote sensing and modeled chlorophyll-a products of the Baltic Sea. *J. Appl. Remote Sens.* **2022**, *16*, 046516. [CrossRef]
59. Karlson, A.M.L.; Duberg, J.; Motwani, N.H.; Hogfors, H.; Klawonn, I.; Ploug, H.; Sveden, J.B.; Garbaras, A.; Sundelin, B.; Hajdu, S.; et al. Nitrogen fixation by cyanobacteria stimulates production in Baltic food webs. *Ambio* **2015**, *44*, 413–426. [CrossRef]
60. Olofsson, M.; Klawonn, I.; Karlson, B. Nitrogen fixation estimates for the Baltic Sea indicate high rates for the previously overlooked Bothnian Sea. *Ambio* **2021**, *50*, 203–214. [CrossRef] [PubMed]
61. Alikas, K.; Kangro, K.; Reinart, A. Detecting cyanobacterial blooms in large North European lakes using the maximum chlorophyll index. *Oceanologia* **2010**, *52*, 237–257. [CrossRef]
62. Nurmik, M.; Eljas, K. Merestrateegia Raamdirektiivi (2008/56/EÜ) Kohase Eesti Mereala Keskkonnaseisundi Hinnangu Indikaatorite Kogum. 2018. Available online: www.klab.ee (accessed on 10 July 2023).
63. Klauson, A.; Lotman, A.; Jaanus, A.; Kuus, A.; Põllumäe, A.; Martin, G.; Ojaveer, H.; Taal, I.; Lips, I.; Jüssi, I.; et al. Eesti Mereala Keskkonnaseisund 2018. 2019. Available online: https://shorturl.at/oxA26 (accessed on 10 July 2023).
64. Alikas, K.; Ansko, I.; Vabson, V.; Ansper, A.; Kangro, K.; Uudeberg, K.; Ligi, M. Consistency of radiometric satellite data over lakes and coastal waters with local field measurements. *Remote Sens.* **2020**, *12*, 616. [CrossRef]
65. Windle, A.E.; Evers-King, H.; Loveday, B.R.; Ondrusek, M.; Silsbe, G.M. Evaluating Atmospheric Correction Algorithms Applied to OLCI Sentinel-3 Data of Chesapeake Bay Waters. *Remote Sens.* **2022**, *14*, 1881. [CrossRef]
66. Warren, M.A.; Simis, S.G.H.; Martinez-Vicente, V.; Poser, K.; Bresciani, M.; Alikas, K.; Spyrakos, E.; Giardino, C.; Ansper, A. Assessment of atmospheric correction algorithms for the Sentinel-2A Multispectral Imager over coastal and inland waters. *Remote Sens. Environ.* **2019**, *225*, 267–289. [CrossRef]
67. Soomets, T.; Uudeberg, K.; Jakovels, D.; Brauns, A.; Zagars, M.; Kutser, T. Validation and comparison of water quality products in baltic lakes using sentinel-2 msi and sentinel-3 OLCI data. *Sensors* **2020**, *20*, 742. [CrossRef]
68. Kutser, T.; Paavel, B.; Metsamaa, L.; Vahtmä, E. Mapping coloured dissolved organic matter concentration in coastal waters. *Int. J. Remote Sens.* **2009**, *30*, 5843–5849. [CrossRef]
69. Gower, J.; King, S.; Young, E. Global remote sensing of Trichodesmium. *Int. J. Remote Sens.* **2014**, *35*, 5459–5466. [CrossRef]
70. Gower, J.; King, S.; Goncalves, P. New results from a global survey using MERIS MCI. *Int. J. Remote Sens.* **2008**, *21*, 6209–6216. [CrossRef]
71. Alikas, K.; Kratzer, S. Improved retrieval of Secchi depth for optically-complex waters using remote sensing data. *Ecol. Indic.* **2017**, *77*, 218–227. [CrossRef]
72. Konik, M.; Bradtke, K.; Stoń-Egiert, J.; Soja-Woźniak, M.; Śliwińska-Wilczewska, S.; Darecki, M. Cyanobacteria Index as a Tool for the Satellite Detection of Cyanobacteria Blooms in the Baltic Sea. *Remote Sens.* **2023**, *15*, 1601. [CrossRef]
73. Clark, J.M.; Schaeffer, B.A.; Darling, J.A.; Urquhart, E.A.; Johnston, J.M.; Ignatius, A.R.; Hyer, M.H.; Loftin, K.A.; Werdell, J.; Stumpf, R.P. Satellite monitoring of cyanobacterial harmful algal bloom frequency in recreational waters and drinking water sources. *Ecol. Indic.* **2017**, *80*, 84–95. [CrossRef]
74. Mishra, S.; Stumpf, R.P.; Schaeffer, B.A.; Werdell, P.J.; Loftin, K.A.; Meredith, A. Measurement of Cyanobacterial Bloom Magnitude using Satellite Remote Sensing. *Sci. Rep.* **2019**, *9*, 18310. [CrossRef]
75. Uudeberg, K.; Aavaste, A.; Kõks, K.-L.; Ansper, A.; Uusõue, M.; Kangro, K.; Ansko, I.; Ligi, M.; Toming, K.; Reinart, A. Optical water type guided approach to estimate optical water quality parameters. *Remote Sens.* **2020**, *12*, 931. [CrossRef]
76. Kowalczuk, P. Seasonal variability of yellow substance absorption in the surface layer of the Baltic Sea. *J. Geophys. Res. Ocean.* **1999**, *104*, 30047–30058. [CrossRef]
77. Harvey, E.T.; Kratzer, S.; Andersson, A. Relationships between colored dissolved organic matter and dissolved organic carbon in different coastal gradients of the Baltic Sea. *Ambit* **2015**, *44*, 392–401. [CrossRef] [PubMed]
78. Paavel, B.; Arst, H.; Metsamaa, L.; Toming, K.; Reinart, A. Optical investigations of CDOM-rich coastal waters in Pärnu Bay. *Est. J. Earth Sci.* **2011**, *60*, 102–112. [CrossRef]
79. Wasmund, N. Occurrence of cyanobacterial blooms in the baltic sea in relation to environmental conditions. *Int. Rev. Gesamten Hydrobiol.* **1997**, *82*, 169–184. [CrossRef]
80. Wasmund, N.; Nausch, G.; Voss, M. Upwelling events may cause cyanobacteria blooms in the Baltic Sea. *J. Mar. Syst.* **2012**, *90*, 67–76. [CrossRef]
81. Nausch, M.; Nausch, G.; Lass, H.U.; Morholz, V.; Nagel, K.; Siegel, H.; Wasmund, N. Phosphorus input by upwelling in the eastern Gotland Basin (Baltic Sea) in summer and its effects on filamentous cyanobacteria. *Estuararine Coast. Shelf Sci.* **2009**, *83*, 434–442. [CrossRef]
82. Vahtera, E.; Laanemets, J.; Pavelson, J.; Huttunen, M.; Kononen, K. Effect of upwelling on the pelagic environment and bloom-forming cyanobacteria in the western Gulf of Finland, Baltic Sea. *J. Mar. Syst.* **2005**, *58*, 67–82. [CrossRef]

83. Estonian Environment Agency. *MERESEIRE 2022 ARUANNE OSA 2. Rannikumere Seire*; Unpublished Work; Estonian Environment Agency: Tallinn, Estonia, 2023.
84. O'Neil, J.M.; Davis, T.W.; Burford, M.A.; Gobler, C.J. The rise of harmful cyanobacteria blooms: The potential roles of eutrophication and climate change. *Harmful Algae* **2012**, *14*, 313–334. [CrossRef]
85. Woźniak, M.; Bradtke, K.M.; Darecki, M.; Krężel, A. Empirical model for phycocyanin concentration estimation as an indicator of cyanobacterial bloom in the optically complex coastal waters of the baltic sea. *Remote Sens.* **2016**, *8*, 212. [CrossRef]
86. Riddick, C.A.L.; Hunter, P.D.; Gomez, J.A.D.; Martinez-Vicente, V.; Presing, M.; Horvath, H.; Kovacs, A.W.; Vörös, L.; Zsigmond, E.; Tyler, A.N. Optimal cyanobacterial pigment retrieval from ocean colour sensors in a highly turbid, optically complex lake. *Remote Sens.* **2019**, *11*, 1613. [CrossRef]
87. Ogashawara, I. Determination of phycocyanin from space—A bibliometric analysis. *Remote Sens.* **2020**, *12*, 567. [CrossRef]
88. Spisla, C.; Taucher, J.; Bach, L.T.; Haunost, M.; Boxhammer, T.; King, A.L.; Jenkins, B.D.; Wallace, J.R.; Ludwig, A.; Meyer, J.; et al. Extreme Levels of Ocean Acidification Restructure the Plankton Community and Biogeochemistry of a Temperate Coastal Ecosystem: A Mesocosm Study. *Front. Mar. Sci.* **2021**, *7*, 611157. [CrossRef]
89. Ullah, H.; Nagelkerken, I.; Goldenberg, S.U.; Fordham, D.A. Climate change could drive marine food web collapse through altered trophic flows and cyanobacterial proliferation. *PLoS Biol.* **2018**, *16*, e2003446. [CrossRef] [PubMed]

Disclaimer/Publisher's Note: The statements, opinions and data contained in all publications are solely those of the individual author(s) and contributor(s) and not of MDPI and/or the editor(s). MDPI and/or the editor(s) disclaim responsibility for any injury to people or property resulting from any ideas, methods, instructions or products referred to in the content.